

# UC Davis

## UC Davis Previously Published Works

### Title

Geospatial organization of fluvial landforms in a gravel-cobble river: Beyond the riffle-pool couplet

### Permalink

<https://escholarship.org/uc/item/3761d9th>

### Journal

Geomorphology, 213

### ISSN

0169555X

### Authors

Wyrick, J.R.  
Pasternack, G.B.

### Publication Date

2014-05-01

### DOI

10.1016/j.geomorph.2013.12.040

Peer reviewed

1 Geospatial organization of fluvial landforms in a gravel–cobble river: beyond the riffle–  
2 pool couplet

3

4 J.R. Wyrick and G.B. Pasternack\*

5

6 University of California, Davis, One Shields Drive, Davis, CA 95616, USA

7

8 \* Corresponding author. Tel.: + 1 530-302-5658; Fax: + 1 530-752-5262;

9 E-mail: [gpast@ucdavis.edu](mailto:gpast@ucdavis.edu).

10

11

12

13 **Abstract**

14

15 Morphological units (MU) are landforms with distinct local form–process associations at  
16 ~ 1-10 channel widths scale that may be the fundamental building blocks describing the  
17 geomorphic structure of a river. Past research has disproportionately focused on the  
18 two MUs of pool and riffle, conjecturing that they are the central linked couplet in the  
19 process–form association. The goal of this study was to delineate and map spatially  
20 explicit fluvial landforms in two-dimensional planview within a gravel–cobble bed river  
21 using two-dimensional hydrodynamic delineation and then to statistically examine MU  
22 geospatial patterns for indicators of deterministic geomorphic control. This procedure is  
23 not discharge-dependent like mesohabitat methods, but gets at the geometry of  
24 underlying landforms. Statistical testing confirmed that eight delineated in-channel MU  
25 types comprise a complex and diverse channel morphology in which pools and riffles  
26 are not directly coupled. Specifically, gravel–cobble river channels (1) exhibit  
27 nonrandom spatial organization of their longitudinally and laterally variable landform  
28 morphology; (2) consist of a variety of MU types, not just pools and riffles; and (3) show  
29 distinct MU collocations and avoidances, with riffles linked to chutes and runs, while  
30 pools are linked to slackwaters and glides. Planview MU delineation with two-  
31 dimensional hydrodynamic modeling provides a ‘bottom-up’ approach to understanding  
32 and linking channel morphology with ecosystem services and geomorphic processes  
33 and is being used to guide river management and rehabilitation strategies.

34

35 *Keywords:* morphological unit; channel unit; riffles; pools; river landforms

## 36 1. Introduction

37 A river channel is a complex configuration of morphologies, ranging from the  
38 dendritic drainage networks at the catchment scale to cobble clusters at the centimeter  
39 scale. The spatial patterns of rivers have long intrigued fluvial scientists, and much  
40 literature is available that is focused on the attempt to define and classify these patterns  
41 at all spatial and temporal scales. For the research presented herein, the landforms  
42 within a long channel segment will be analyzed at the morphological unit scale (~ 1-10  
43 channel widths, W).

44 The mapping of river morphology at the 1-10 W scale is common practice for  
45 researchers studying fluvial systems and is well reported in the literature. Several terms  
46 exist for discernible units at this scale, such as *channel unit* (e.g., Grant et al., 1990;  
47 Bisson et al., 1996), *channel geomorphic unit* (e.g., Hawkins et al., 1993), *morphological*  
48 *unit* (e.g., Wadeson, 1994), and *physical biotope* (e.g., Newson and Newson, 2000).  
49 The term *morphological unit* (MU) is used in this study in order to not be confined to just  
50 the channel as well as to avoid imposing any habitat requirement.

51 A review of previous landform studies shows that MUs are typically identified but  
52 then their spatial organization is mostly ignored, with the focus instead on correlations  
53 between individual MU types and channel gradient (Halwas and Church, 2002), how  
54 habitat varies with discharge (e.g., Hauer et al., 2009) or time (e.g., Madej, 2001; Klaar  
55 et al., 2009), their associated hydraulics (e.g., Wadeson and Rowntree, 1998), or using  
56 the units as a basis for segregating biologic data (e.g., Zimmer and Power, 2006;  
57 Schwartz and Herricks, 2008). Among previous studies that did analyze the spatial  
58 organization of MUs, the most common metric reported is that of one-dimensional

59 longitudinal spacing between riffles and pools (e.g., Keller and Melhorn, 1978; Gregory  
60 et al., 1994), which are also usually coupled into a single 'unit' (e.g., Thompson, 1986).  
61 However, one-dimensional studies ignore lateral variability in channel morphology, an  
62 aspect that is key to diverse hydraulics and habitat. A few studies have also reported  
63 abundance percentages and streamwise sequences of unit-to-unit transitions (e.g.,  
64 Grant et al., 1990; Borsanyi et al., 2004).

65 Significant differences in channel delineation exist between biologists and  
66 geomorphologists. When delineating gravel–cobble channels into habitats at the 1-10 W  
67 scale for biologic purposes, a large catalog of unit types and descriptions exists (e.g.,  
68 Maddock, 1999; Newson and Newson, 2000). However, when delineating channels into  
69 MUs for geomorphic purposes, the catalog of commonly published types primarily  
70 reduces to pools and riffles, which are the elevational end members (e.g., O'Neill and  
71 Abrahams, 1984; Thompson, 1986). The spatial patterns of other MUs such as runs,  
72 chutes, and glides might be just as important for assessing the channel complexity and  
73 habitat potential but are rarely investigated (e.g., Grant et al., 1990; Moir and  
74 Pasternack, 2008). This study delineated eight distinct MUs and evaluated the spatial  
75 organization of all of them with respect to the channel segment and to each other.

76 The spatial heterogeneity of fluvial landforms is important to ascertain because it can  
77 be an indicator of the 'health' of a river. High complexity of landforms generally equates  
78 to high diversity of hydraulics and thus high biodiversity across all ecologic lifestages  
79 (e.g., Frissell et al., 1986; Newson and Newson, 2000), although Newson and Large  
80 (2006) do caution against a pure correlation of only equating geodiversity to biodiversity  
81 from a habitat management viewpoint. However, geodiversity in fluvial landforms does

82 at least set a framework for habitat protection and conservation (Gray, 2004), and thus  
83 evaluation of the channel at the 1-10 W scale is key to assessing the physical habitat  
84 (Maddock, 1999). As an example of this correlation, Reid et al. (2008) showed that poor  
85 habitat conditions of river reaches are generally associated with a low diversity of MUs.  
86 Channel complexity should ideally be described by the composition and the  
87 configuration of MUs, where a highly complex channel would exhibit statistically  
88 nonrandom patterns for each metric, with examples of such tests developed and  
89 provided herein.

90 The debate over the appropriate number and definitions of fluvial landforms is far  
91 from over, and there is especially a lack of published studies that analyze landforms  
92 within a planview geospatial context. The goal of this study was thus to delineate and  
93 map fluvial landforms of a gravel–cobble bed river as objectively as possible aided with  
94 two-dimensional (2D) hydrodynamic modeling and then to statistically examine  
95 geospatial patterns for indicators of systematic geomorphic control. The results  
96 presented herein illustrate how complex and diverse a channel's morphology can be.

97

## 98 **2. Study site**

99 The Yuba River is a tributary of the Feather River in north-central California, USA,  
100 that drains 3480 km<sup>2</sup> of the western Sierra Nevada range (Fig. 1). The watershed has a  
101 history of hydraulic mining that is the source of the present alluvium. Englebright Dam  
102 was built in 1940 to trap nearly all sediment and thereby promote downstream  
103 geomorphic recovery, which continues to proceed more than 70 years later (Carley et  
104 al., 2012). Daguerre Point Dam (DPD) is an 8-m high irrigation diversion structure

105 located at river kilometre (RKM) 17.8 that creates a slope break and partial sediment  
106 barrier. Instantaneous stage-discharge has been continuously recorded at the USGS  
107 gages at Smartsville near Englebright Dam (#11418000), at Marysville near the mouth  
108 (#11421000) (Fig. 1), and on the regulated tributary Deer Creek (#11418500). Base flow  
109 typically occurs during the late fall season when Chinook (*Oncorhynchus tshawytscha*)  
110 adults spawn.

111 The 37.1-km river segment between Englebright Dam and the Feather River  
112 confluence is defined as the lower Yuba River (LYR). The LYR is a single-thread  
113 channel (~ 20 emergent bars/islands at bankfull) with low sinuosity, high width-to-depth  
114 ratio, and slight to no entrenchment. The geomorphically determined bankfull discharge  
115 was estimated as 141.6 m<sup>3</sup>/s, which has ~ 82% annual exceedance probability. The  
116 river corridor is confined in a steep-walled bedrock canyon for the upper 3.1 RKM, then  
117 transitions first into a wider bedrock valley with some meandering through Timbuctoo  
118 Bend (RKM 28.3-34.0; Fig. 1), then into a wide, alluvial valley downstream to the mouth.  
119 Hydraulic mining sediment was used to train the active river corridor in the wide  
120 lowlands to isolate it from the ~ 4,000 ha Yuba Goldfields. Riverbed thalweg elevations  
121 range from ~ 9 to 88 m above mean sea level (NAVD88 datum), with a mean bed slope  
122 of 0.185%. The segment-scale mean diameter of the channel sediment is 97 mm (i.e.,  
123 small cobble). In the bedrock canyon just below Englebright Dam, the mean wetted  
124 width at base-flow discharge is 36.4 m. The remainder of the base-flow channel  
125 upstream of DPD widens to a mean wetted width of 64.6 m, and then the channel below  
126 DPD narrows slightly to a mean wetted width of 56.4 m. At bankfull, the mean widths  
127 are 51.4, 99.4, and 98.4 m, respectively, for those same regions. As a comparison to

128 other rivers, the LYR is classified as a C3 channel by the Stream Type classification  
129 method (Rosgen, 1996) and as transitional between straight and meandering by the  
130 flow instability method (Parker, 1976). Existing literature with more information about the  
131 hydrogeomorphic conditions of the LYR includes Pasternack (2008), Moir and  
132 Pasternack (2008, 2010), James et al. (2009), Sawyer et al. (2010), White et al. (2010),  
133 Wyrick and Pasternack (2012), and Abu-Aly et al. (2013).

134

### 135 **3. Physical data collection**

#### 136 *3.1. Topographic and bathymetric mapping*

137 River corridor topography and bathymetry were collected for the high resolution  
138 digital elevation model (DEM) using a combination of ground-based, boat-based, and  
139 remote sensing methods in accordance with a predesigned protocol (Pasternack, 2009;  
140 Carley et al., 2012). Different regions were mapped at different times between 2006 and  
141 2009 as funding permitted. Each survey method involved its own internal performance  
142 tests, such as backsight checks, GPS root mean square values, and comparison of  
143 airborne Light Detection and Ranging (LiDAR) observations to ground-based  
144 observations on flat, smooth roads. The only gap in the DEM is the Narrows Reach  
145 (RKM ~ 34-36), which contains unwadable, unboatable, air bubble-prolific, and therefore  
146 unsurveyable rapids. On 21 September 2008, Aero-Metric, Inc. (Seattle, WA) acquired  
147 LiDAR bare earth elevations of the river corridor during a constant low flow typical of the  
148 period when hydro facility maintenance takes place: 24.4 m<sup>3</sup>/s between Englebright  
149 Dam and DPD and 17.6 m<sup>3</sup>/s below DPD where irrigation diversions occur. A  
150 professional hydrography firm (Environmental Data Solutions, San Rafael, CA) collected



151 bathymetric points along longitudinal and cross-channel lines, meeting class 1 standard  
152 ( $\pm 0.5$  feet vertical accuracy). Because some areas were inaccessible by boat or were  
153 easier to map by wading, ground crews surveyed sections of the channel with either a  
154 robotic total station (Leica TPS1200) or a real-time kinetic (RTK) GPS (Trimble R7). All  
155 of the different surveys were tied together with a common array of benchmarks and  
156 vertical adjustment to a common vertical datum (NAVD 88). The resulting reach-  
157 averaged topographic point density ranged from 28 to 60 and from 11 to 554 points/100  
158  $m^2$  within and beyond the  $24.92 m^3/s$  base-flow domain, respectively. Low densities are  
159 associated with ground-based surveys.

160 Quality assurance and quality control procedures were applied to the field data, and  
161 then a DEM was produced. Data from every different survey was compared against  
162 every other method at overlaps to assess uncertainty. For example, a comparison of  
163 boat-based water surface elevations versus those from ground-based RTK GPS at the  
164 adjacent water's edge yielded observed vertical differences of 75% of test points within  
165 3 cm, 91% within 6 cm, and 99% within 15 cm. After accounting for data quality,  
166 acceptable points were visualized in ArcGIS software (ESRI, Redlands, CA) and further  
167 edited on a spatial basis to remove obvious errors. In narrow backwater channels and  
168 along banks that contained obvious interpolation errors, hydro-enforced breaklines and  
169 regular breaklines were created to better represent landform features. Additionally,  
170 some bathymetric areas that contained very few points because of obstructions and  
171 other problematic features were artificially augmented, so that channel characteristics  
172 were maintained. A TIN-based DEM was produced as the native terrain model from  
173 which derivative rasters and contours were produced as needed.

174

175 *3.2. Two-dimensional hydrodynamic model*

176 The surface-water modeling system (Aquaveo, LLC, Provo, UT) and sedimentation  
177 and river hydraulics–two-dimensional (SRH-2D; Lai, 2008) were used to produce 2D  
178 hydrodynamic models of the LYR according to the procedures of Pasternack (2011).  
179 This model has a 2D finite-volume solver for depth-averaged shallow water equations to  
180 estimate depth and velocity at each computational node. Details about the LYR 2D  
181 model are in Barker (2011), Abu-Aly et al. (2013), and Pasternack et al. (2013).  
182 Because the LYR 2D model is a local management tool, it was built in English units, so  
183 reported values herein using SI units may seem unusual. This study only used  
184 simulations for base flows of 15.01 and 24.92 m<sup>3</sup>/s, as well as the geomorphically  
185 determined bankfull flow of 141.58 m<sup>3</sup>/s. The typical internodal spacing of each  
186 computational mesh for this range of flows was either 0.91 or 1.5 m. Input discharge  
187 was obtained from the USGS stations listed in section 2, accounting for agricultural  
188 diversion at DPD. Water surface elevations at the exit of each model domain for base  
189 flow were directly surveyed, while those for bankfull discharges were either surveyed or  
190 obtained from rating curves made with automated water-level loggers.

191 Boundary roughness was partially addressed by creating a highly detailed DEM, with  
192 unresolved roughness addressed by using a constant Manning's roughness value ( $n$ )  
193 for unvegetated terrain in each reach. Past site-scale 2D model studies on the LYR  
194 used an  $n$  of 0.043 for the unvegetated, gravel–cobble riverbed (Moir and Pasternack,  
195 2008; Sawyer et al., 2010). For the long model domains in this study, an evaluation of  
196 observed and modeled water surface elevations at a range of in-channel flows up to

197 bankfull found that an  $n$  of 0.04 was best downstream of DPD, an  $n$  of 0.032 best for the  
198 bedrock canyon below Englebright Dam, and an  $n$  of 0.03 best for the valley-confined  
199 Timbuctoo Bend (Pasternack et al., 2013). Based on LiDAR mapping of the vegetation  
200 canopy, the area of vegetation at base flow was  $< 4\%$  and likely consisted of  
201 overhanging canopy, so vegetation was not quantified in boundary roughness. At  
202 bankfull discharge, indicators of boundary roughness showed no difference from that at  
203 base flow, so the same unvegetated  $n$  values were used.

204 The suitability of the constant roughness values (among other model aspects) was  
205 carefully tested by model validation using independent data spanning an order of  
206 magnitude of discharge ( $\sim 14$  to  $170 \text{ m}^3/\text{s}$ ). Full model validation details were reported in  
207 Barker (2011). Mass conservation between specified input flow and computed output  
208 flows was within 1%. Water surface elevation performance can be evaluated relative to  
209 a river's mean substrate size because grain-scale topographic variation and water  
210 surface fluctuations limit WSE observation accuracy. For the LYR, the mean substrate  
211 size was  $\sim 10 \text{ cm}$  (Wyrick and Pasternack, 2012). The mean signed vertical deviation  
212 for 197 observations at  $24.92 \text{ m}^3/\text{s}$  was  $-1.8 \text{ mm}$ . For unsigned deviations (i.e., absolute  
213 values), 27% were within 3.1 cm vertical, 49% of deviations within 7.62 cm, 70% within  
214 15.25 cm, and 94% within 30.5 cm. From cross-sectional surveys yielding 199  
215 observations, predicted versus observed depths yielded a good coefficient of  
216 determination ( $r^2$ ) of 0.66. Using Lagrangian tracking of an RTK GPS on a floating  
217 kayak, surface velocity magnitude was measured by Barker (2011) at 5780 locations,  
218 yielding a very good predicted versus observed  $r^2$  of 0.79. Median unsigned velocity  
219 magnitude error was 16%, which is less than commonly reported. Using Lagrangian

220 tracking of an RTK GPS on a floating kayak, velocity direction was also tested at those  
221 5780 points, yielding a predicted versus observed  $r^2$  of 0.80. This parameter is not  
222 commonly tested, but likely should be for 2D models. Median direction error was 4%,  
223 with 61% of deviations within 5° and 86% of deviations within 10°. Overall, the LYR 2D  
224 model met or exceeded all common standards of 2D model performance.

225

#### 226 **4. Morphological unit map**

227 To identify and delineate the MUs, base-flow hydraulics were used to infer  
228 underlying channel morphology. Specific geomorphic landforms were assumed to  
229 exhibit discrete combinations of depth and velocity at a representative base flow. A  
230 complete and contiguous map of MUs was obtained from two inputs: (i) spatial grids of  
231 depth and velocity at a low steady discharge (when topography is the primary control on  
232 hydraulics) estimated using a 2D hydrodynamic model, and (ii) an expert-specified MU  
233 classification scheme using depth and velocity threshold values. With these inputs, all  
234 raster pixels were objectively classified into an MU type with a GIS-based algorithm,  
235 and then coherent MUs were identified as adjacent aggregates of individually classified  
236 points.

237 The channel bed within the base-flow wetted area was delineated into contiguous  
238 polygons of coherent landforms using a six-step procedure (Fig. 2) following the  
239 methodology presented in more detail in Pasternack (2011) and Wyrick and Pasternack  
240 (2012). First, detailed topographic and bathymetric data of the LYR were obtained and a  
241 DEM was produced (section 3.1). Second, expert judgment and local knowledge  
242 (guided from observations during data collection) were used to predetermine the

243 number and nomenclature of MU types to be mapped, and then the range of each  
244 hydraulic variable was estimated for each MU type. Hydraulic thresholds were codified  
245 into an algorithm for classifying individual raster cells. Third, an appropriate low flow  
246 regime was identified at which to delineate MUs. Fourth, a 2D hydrodynamic model was  
247 developed, run, and validated for MU delineation at the LYR base flow (section 3.2).  
248 Fifth, rasters of the key delineation variables (i.e., depth and velocity) were created  
249 consistent with the resolution of the 2D model. Sixth, the objective MU delineation  
250 algorithm was applied to obtain a preliminary MU map. Lastly, the MU map was  
251 reviewed and evaluated by a diverse team of LYR experts to determine whether the MU  
252 types and hydraulic thresholds used in the process yielded meaningful patterns.

253

#### 254 *4.1. Base flow selection*

255 For the LYR, controllable flows are set by flow schedules in the Lower Yuba Accord  
256 Fisheries Agreement (2007), but often enough flow occurs to operate above minimum  
257 requirements. A typical base-flow regime consists of  $\sim 24.92 \text{ m}^3/\text{s}$  ( $\sim 0.18$  times  
258 bankfull) out of Englebright Dam, no discharge out of either of the two tributaries (whose  
259 outflows are normally  $0\text{--}0.142 \text{ m}^3/\text{s}$  when the LYR is at base flow), and a societal  
260 withdrawal of  $9.91 \text{ m}^3/\text{s}$  of water at Daguerre Point Dam (DPD), yielding a Marysville  
261 gage flow of  $15.01 \text{ m}^3/\text{s}$ . Because of this withdrawal, a paired discharge regime is  
262 appropriate to use here (i.e., combining model results for  $24.92 \text{ m}^3/\text{s}$  above DPD with  
263  $15.01 \text{ m}^3/\text{s}$  results below DPD) for MU mapping to account for the diversion, instead of  
264 using a theoretical constant discharge for the whole river. The selected base-flow  
265 discharges are equivalent to  $\sim 75\%$  daily exceedance probability.

266 The methodology of delineating MUs is robust enough that the resultant map is not  
267 sensitive to the selected base-flow discharge. When carefully analyzed for procedures  
268 and assumptions, virtually all landform mapping methods that exist today have a  
269 hydraulic dependency, including methods that use topographic longitudinal profiles. In  
270 the approach used in this study, experts establish which landforms are indicated by  
271 each range of depth and velocity at the selected discharge. Sensitivity analysis by  
272 Wyrick and Pasternack (2012) found that fixed hydraulic thresholds accurately reflect  
273 underlying topography for discharge variations within  $\sim \pm 15\%$ . However, there is no  
274 sensitivity limit when thresholds are adjusted by experts to the modeled discharge.  
275 Thus, reliance on hydraulics does not mean that the methodology only captures  
276 discharge-dependent habitats; it actually does get at underlying landforms.

277

#### 278 *4.2. MU names and definitions*

279 Moir and Pasternack (2008) previously created a hand-drawn MU map for a 457-m-  
280 long site on the LYR at the apex of Timbuctoo Bend (Fig. 1) guided by field experience,  
281 a DEM, and hydraulic rasters. This MU map, despite its subjectivity, provided thoughtful  
282 expert opinion and thus was a useful guide in selecting hydraulic metrics for the full LYR  
283 segment. Building from their study, Pasternack (2008) made an incremental  
284 improvement by using objective depth and topographic indicators along with subjective  
285 velocity estimates to map the MUs in all of Timbuctoo Bend, including several additional  
286 MU types that were not used in the initial site by Moir and Pasternack (2008). Building  
287 on Pasternack (2008) and drawing on commonly accepted descriptions, the MUs were  
288 identified, defined, and delineated for this study (Table 1, wherein descriptions of depth

289 and velocity refer to those that are created by the landforms during the base-flow  
290 discharge used for this analysis).

291

#### 292 *4.3. MU mapping process*

293 The resultant hydraulic rasters (0.91 x 0.91 m<sup>2</sup>) were used to delineate eight in-  
294 channel MUs based on quantitative thresholds of depth and velocity (Fig. 3) in ArcGIS.  
295 Initial threshold values were based on and manipulated from the MU maps of Moir and  
296 Pasternack (2008) and Pasternack (2008). The resulting trial pattern was overlain on  
297 National Agricultural Image Program (NAIP) imagery. A visual inspection of the imagery  
298 was made by a group of LYR biologists, engineers, and geomorphologists with  
299 extensive ground-based experience. Their assessments were used to determine if the  
300 trial MU pattern conceptually conformed to the kind of MU delineation that would be  
301 yielded solely by subjective expert geomorphological opinion. These deliberations were  
302 not used to check or evaluate exact boundaries, however, which are more precisely  
303 specified by the computer algorithm than by eye or GPS. An iterative process of  
304 consensus-based adjustment to MU names, definitions, and thresholds led to the final  
305 set of depth and velocity threshold values (Fig. 3).

306

#### 307 **5. Spatial pattern analysis methods**

308 MU spatial organization was analyzed from a segment-scale perspective. Statistical  
309 comparisons were derived from evaluating the organization of each MU type against the  
310 others and incorporating them into a broader context of geomorphic concepts. Overall  
311 composition and organization comparisons of the LYR against other specific rivers

312 require more applications of this new methodology. For this study, the analyses focused  
313 on the sizes of polygons of each MU type and the diversity of polygon sizes amongst all  
314 MUs, which then guide an analysis to determine the minimum size of an MU that is  
315 statistically relevant and readily identifiable in the field. The remaining spatial analyses  
316 then include duplicate analyses and discussions in which all delineated polygons were  
317 used versus using only those that satisfy the minimum size criteria. The spatial analyses  
318 investigated to characterize MU organization include longitudinal distributions,  
319 longitudinal spacings between individuals of a given MU type, nondirectional adjacency  
320 collocations and avoidances between MU types, and the lateral abundance and  
321 variability of MUs at any given cross section. The locations of MUs are also placed in  
322 context with such hydromorphic characteristics as water surface slope, base-flow  
323 wetted width, and bankfull width–depth ratios.

324

### 325 *5.1. Abundance and diversity*

326 Previous MU studies reported total number of unique unit types, but not all quantify  
327 the total number and spatial coverage of each unit type compared against the others.  
328 This metric is important for assessing whether one or a few types tend to dominate the  
329 channel. If MUs randomly occur, no MU type would dominate and any particular location  
330 would have equal probability of becoming any MU. The total areas of each MU would  
331 therefore be equal to  $100/n\%$ , where  $n$  is the number of MU types specific to that river  
332 segment. Note that no known deterministic mechanism yet exists to yield uniform MU  
333 abundance among types.



334 To calculate the abundance of each MU type in the LYR, the area of each individual  
335 MU was calculated in ArcGIS. Polygon areas were summed by MU type and divided by  
336 the total wetted area to determine percent coverage. Additionally, histograms of polygon  
337 area were plotted for each MU type and compared among types.

338 The Shannon Diversity Index is a common method utilized to quantify the spatial  
339 complexity and heterogeneity of habitat but has also been applied to MUs (Maddock et  
340 al., 2008). Assessments of diversity ( $H$ ), evenness ( $J$ ), and dominance ( $D$ ) of the total  
341 MU areas were calculated with the following equations:

$$342 \quad H = -\sum(p_i \times \ln p_i) \quad (1)$$

$$343 \quad J = H/\ln(N) \quad (2)$$

$$344 \quad D = \ln(N) - H \quad (3)$$

345 where  $p_i$  is the fraction of total wetted area of the  $i$ -th MU type, and  $N$  is the total number  
346 of MU types. For the eight MU types in the LYR, a fully diverse composition would  
347 exhibit equal areas of each type (i.e.,  $p_i = 1/8 = 0.125$ ), a diversity index of 2.079, an  
348 evenness of 1.0, and a dominance factor of 0.0.

349

## 350 *5.2. Longitudinal distribution*

351 An important question is whether MUs are spatially organized or randomly located  
352 along a river segment. Most scientists assume they are organized, but that needs to be  
353 quantified for 2D MUs. By definition, if they are randomly located, then any particular  
354 location would have equal probability of being any MU. When that is the case, then the  
355 type of statistical distribution that is present is called a uniform distribution. No known  
356 deterministic mechanism yet exists to yield a uniform MU longitudinal distribution. The

357 presence of a uniform distribution is indicated by having a horizontal discrete probability  
358 distribution function (PDF) and a diagonal straight-line cumulative distribution function  
359 (CDF) when probability of occurrence is plotted against channel distance. In a CDF,  
360 deviations of the slope from a straight-line trajectory indicate a higher or lower  
361 occurrence in a region of channel relative to the uniform expectation, where a steeper  
362 slope would indicate a higher occurrence and a lower slope would indicate a lower  
363 occurrence. Plotting the longitudinal distribution of the MUs shows whether a particular  
364 MU type tends to cluster in some regions of the channel or not.

365 The longitudinal distributions herein were calculated as the percent area of each MU  
366 type among all cross sections. Using ArcGIS, the river valley centerline was  
367 automatically stationed and given perpendicular cross sections evenly every 6 m (~ 1/10  
368 base-flow width) along the study segment. Cross sections were then buffered 3 m  
369 upstream and downstream to create rectangles that spanned the wetted width and  
370 contiguously covered the segment area (see Fig. 4 for an example). Within each  
371 rectangle, the areas of each MU type were calculated and converted to a percent of  
372 total MU type area, and those areas were assigned to the cross section at each  
373 rectangle's center. Longitudinal distributions are presented as both discrete and  
374 cumulative area functions.

375

### 376 *5.3. Longitudinal spacing*

377 A commonly accepted notion in fluvial geomorphology is that longitudinal pool-riffle  
378 spacing is ~ 5-7 channel widths (W), as first postulated by Leopold et al. (1964) and  
379 supported by subsequent studies (e.g., Keller, 1972; Richards, 1976; Gregory et al.,

1994). However, Keller (1972) reported that even though the mean spacing within his observed rivers was 5-7 W, the modes tended to be less (~ 3-5 W), which may be the result of the channel not being fully developed. O'Neill and Abrahams (1984) also calculated a mean spacing between riffles and pools to be within the 5-7 W range, but with a mode of ~ 3 W, which depended on their tolerance value of what they defined as a bedform. Other studies have also measured distances between riffles and pools in alluvial and mountain streams and found closer groupings than traditional values (i.e., < 5 W). For example, Carling and Orr (2000) found that riffle crests developed about once every 3 W in an alluvial channel and Montgomery et al. (1995) described pool spacings of ~ 2-5 W that were forced by logjams within steep channels. In short, while the commonly expressed spacing value between riffles or pools is 5-7 W, this is clearly not a universal value and deviances from this spacing could provide some insight into the channel's development.

Additionally, even though the spacings between successive units have received considerable attention in the literature, the focus has only been on riffles and pools. In fact, even though Grant et al. (1990) identified and mapped five different channel unit types and analyzed their spatial organization, they only reported longitudinal spacing values for pools because of this lack of other studies with which to compare. This study thus evaluated the longitudinal spacings of all MUs that are longitudinally discrete as a start to the scientific dialogue for other landforms.

In ArcGIS, the centroid of each MU polygon in the LYR was determined and located perpendicularly to the nearest point along the channel's base-flow thalweg. The distances along the thalweg for adjacent points of like MUs were then calculated.

403 Spacing analyses were performed in only the streamwise dimension; therefore, laterally  
404 adjacent units of the same type were not counted as separate units. The example site in  
405 Fig. 5 shows two riffle transition units located on the same cross section but on opposite  
406 banks of the channel. For analysis purposes, these two units were located to the same  
407 thalweg point and therefore only counted as one 'unit' in the calculations. Additionally,  
408 noncontiguous assemblages of the same type that are separated by pixilation effects  
409 were lumped as one discrete unit. Therefore, some discretion had to be employed to  
410 manually exempt some of the units from calculations. Because of this manual  
411 exemption, the statistical analysis was not performed using only those MUs larger than  
412 the minimum size threshold. The distances were then normalized by the mean bankfull  
413 channel width, which is consistent with what Keller (1972) reported.

414

#### 415 *5.4. Adjacency*

416 An underutilized approach to investigating morphological unit organization is the  
417 transition probability analysis method of Grant et al. (1990). This approach evaluates  
418 the frequency that each morphological unit is adjacent to every other unit and then  
419 compares that against the expectation associated with a random system. This approach  
420 should become more valuable now that detailed spatial data sets of fluvial landforms  
421 are becoming readily available. As a result of lack of use, no baseline yet exists as to  
422 what constitutes a 'normal' transition probability matrix, so an important first step is to  
423 apply the method for diverse natural and regulated streams and derive that. Another  
424 important metric is to identify particular preferential combinations that may represent  
425 complex morphological sites at a scale larger than the individual MUs.

426 Because the MU conceptualization used in this study involves lateral and  
427 longitudinal adjacency of units, a new procedure had to be developed to investigate  
428 transition probabilities, which in this analysis become nondirectional adjacency  
429 probabilities. The numbers of common boundaries between two separate MU types  
430 were counted. This type of adjacency is not necessarily one-to-one, however. That is,  
431 unit type A can be adjacent to X number of unit type B, while unit B can be adjacent to  
432 unit type A, a different Y number of times (Fig. 6). That happens because a single type  
433 A polygon can be long and touch multiple type B polygons, whereas in the inverse, all  
434 those B polygons are only touching the one type A polygon. In other words, this method  
435 does not count each individual transition, which would have to be one-to-one, but  
436 instead the metric that is counted is the number of unique adjacencies. As exemplified  
437 in Fig. 6, if three unit B polygons touch the same unit A polygon, then that counts as one  
438 adjacency for B to A, but in the inverse it counts as three adjacencies.

439 The way Grant et al. (1990) evaluated the likelihood that the transition probabilities  
440 were nonrandom was to randomly generate a sequence of units (with each unit equally  
441 likely to occur next in order of selection), calculate the random transition probabilities,  
442 and then compare the real transition probabilities to those. A possible issue with that  
443 method is that the outcome is sensitive to the specific sequence created at random.  
444 Conceivably, one could repeat the step several times and compare the real transition  
445 probabilities to the average of random ones. However, if one were to use a near infinite  
446 number of random sequences, then in the limit, by definition, the transition probabilities  
447 available for this analysis must converge on  $1/N$ , where  $N$  is the number of unit types,  
448 as an equal probability exists of any unit type randomly going to any of the other unit

449 types. As a result, the natural tendency for adjacency to a unit type can be designated  
450 as a *collocation* (analogous to a *preference* for an organism, but recognizing that MUs  
451 are inanimate) on the basis of whether the percent of adjacencies to it are higher than  
452  $1/N$ . Similarly, a natural *avoidance* to adjacency occurs when the percent of adjacencies  
453 are lower than  $1/N$ .

454 Utilizing tools in ArcGIS, the number of adjacencies in the LYR from one MU to  
455 another was counted. The process was repeated for all possible unit-to-unit  
456 combinations. The total number of adjacencies for a particular unit was summed, and  
457 the adjacencies for individual units were represented as percentages of that total. For  
458 the eight MU types in the LYR, the convergence value would be  $1/8$ , or 12.5%. Each  
459 transition probability was then divided by this random percentage to create a matrix that  
460 deviates around a value of one. Adjacencies within 20% of this random value (i.e., 0.8-  
461 1.2) were considered *near-random*.

### 463 5.5. Lateral variability

464 Traditional research usually only considers spatial organization in one dimension,  
465 i.e., one MU per cross section (e.g., O'Neill and Abrahams, 1984; Grant et al., 1990).  
466 However, recent studies have shown that wide rivers exhibit natural lateral variability in  
467 form–process associations (e.g., Bisson et al., 1996; Borsanyi et al., 2004; Moir and  
468 Pasternack, 2008; Milan et al., 2010). To test this hypothesis on the LYR, the number of  
469 distinct MUs at each cross section were counted and compared.

470 This method utilized the same cross-sectional rectangles employed for the  
471 longitudinal analyses. For this approach, the total numbers of unique MU polygons were

472 counted. If one polygon looped out of then back into the same rectangle, it only counted  
473 as one; however, if two separate polygons of the same unit type occurred within the  
474 same rectangle, it counted as two (examples of each of these are illustrated in Fig. 4). If  
475 a polygon spanned multiple cross-sectional rectangles, it would count separately for  
476 each cross section.

477 A wide channel section offers more space for more laterally adjacent MUs (and the  
478 inverse is thus true for narrow sections). So, the raw values could be skewed by  
479 abnormally wide or narrow cross sections. Therefore, results were normalized by the  
480 mean base-flow width by dividing the number of MUs at each cross section by the  
481 actual wetted width at that cross section, and then multiplying by the average width of  
482 the segment's wetted area.

483 A simple count of the total units across each cross section does not create a metric  
484 with which to compare the lateral variability among the MUs, however. Therefore, for  
485 each section that contains a particular MU, the baseflow-width-normalized number of  
486 other MUs were summed and averaged for just those sections. If a unit tends to be  
487 large and dominate its locations, then the count of other MUs per cross section  
488 containing that unit may be low. On the other hand, if a unit tends to be small or slender,  
489 the coincident lateral count could be high.

490

#### 491 *5.6. Hydromorphic characteristics*

492 In an effort to place the MUs in context with the channel geometry, their locations  
493 were compared with three hydromorphic characteristics: base-flow wetted width, water  
494 surface slope, and bankfull width–depth ratio. The water surface slope (WSS) is a key

495 hydraulic feature that has been commonly used as an MU identifier in other studies, and  
496 is a proxy for riverbed slope. Width–depth (W/D) ratios are valuable for expressing  
497 channel hydraulic geometry relationships, as well as indicators of channel stability.

498 In order to relate the hydromorphic characteristics to an MU type, each cross section  
499 needed to be assigned to the MU that dominated it, if one existed. The total areas of  
500 each MU type within each cross-sectional rectangle were determined for the longitudinal  
501 analyses. An MU that consisted of at least 60% of the total area of each cross-sectional  
502 rectangle was considered to be the ‘dominant’ MU for that location. Thus, the mean  
503 hydromorphic characteristics for cross sections dominated by a particular MU type could  
504 be determined. Any cross section that did not exhibit a singular dominant MU was not  
505 used for these analyses.

506 The MU-averaged values were compared between all pairs of MUs using the  
507 nonparametric Mann-Whitney rank-sum U test. This statistical test involves ranking data  
508 and evaluating the sum of the ranks relative to random expectation in assessing the null  
509 hypothesis that two sets of samples come from identical populations (Freund and  
510 Simon, 1991; Pasternack and Brush, 1998). For this study, pairs of MU types were  
511 evaluated for statistical differences above the 99% confidence level ( $p < 0.01$ ), above  
512 the 95% confidence level ( $p < 0.05$ ), and below the 95% confidence level (i.e.,  
513 statistically indifferent).

514 Mean wetted widths were calculated for each cross-sectional rectangle (section 5.2)  
515 and averaged for each type of MU among their respective dominated cross sections.  
516 Each width was then normalized by the segment-scale mean base-flow width.



517 Given variability of MU shapes and sizes, calculating the slope of every individual  
518 unit would not be meaningful, so the MU-dominated cross sections were used. Water  
519 surface elevation (WSE) is a 2D model output that can be converted into a raster.  
520 ArcGIS can then be used to calculate the mean WSE of each cross section. The WSS  
521 at each cross section is calculated as the difference in mean WSE between the two  
522 immediate upstream and downstream cross sections divided by the horizontal distance.  
523 For the case studies presented herein, all WSS values less than zero were removed, as  
524 these were considered to be local anomalies. MU-averaged WSS were thus calculated  
525 from the set of values generated among the representative cross sections for each MU  
526 type.

527 A width–depth ratio  $< 12$  is considered low and  $> 40$  is considered high (*sensu*  
528 Rosgen, 1996). The W/D was calculated based on wetted top width and mean depth  
529 during bankfull flow at each cross section. Cross sections that exhibited a dominant MU  
530 had their W/D ratios tabulated and analyzed, stratified by MU. Thus, the mean W/D ratio  
531 for cross sections dominated by a particular MU type could be determined, as well as  
532 the percent of all MU-dominated cross sections that exhibit a high or low value.

533

## 534 **6. Results**

### 535 *6.1. Abundance and diversity*

536 The MUs in the LYR exhibit an unequal abundance, in total number of polygons and  
537 total area (Table 2). Almost two-thirds of the total numbers of MU polygons were  
538 delineated as either slackwater or slow glide. These high values are likely because the  
539 slackwater and slow glide morphologies are such that they exist along the baseflow  
540 channel margins and therefore are typically long, slender regions that tend to be

541 separated into multiple polygons during the delineation process owing to the square-  
542 pixilation effects. This is supported by the area histograms (Fig. 7) that show slackwater  
543 and slow glides comprise the greatest number of polygons of the smallest possible size  
544 (i.e., one pixel = 0.91 m x 0.91 m) as compared to the other MUs and the fact that these  
545 two units comprise only 28% of the total area (Table 2).

546 In terms of area, the three most abundant units were slackwater, pool, and riffle  
547 transition. Pool covered 15.9% of the segment area, despite having only 2.0% of the  
548 total number of delineated polygons, which indicates that pools are typically delineated  
549 as large cohesive units in the LYR. The three least abundant units in area were chute,  
550 run, and slow glide. Chute and run units also comprised low percentages of the total  
551 number of polygons. Slow glide, however, had the second highest number of polygons,  
552 which indicates that it is typically delineated as small discrete units.

553 Mean polygon sizes ranged from 19 to 404 m<sup>2</sup> for each unit type and maximum  
554 sizes ranged from 7220 to 71,746 m<sup>2</sup> by type (Table 2). Using the mean base-flow  
555 wetted width of 59.5 m, these areas can be normalized into representative length scale  
556 by taking the square root of the area then dividing by the mean flow width. The mean  
557 polygon sizes therefore range between 0.07 and 0.34 W. This calculation assumes a  
558 square unit, even though most of the mapped units in the LYR exhibit an irregular  
559 shape. The maximum size polygons range from 1.43 to 4.50 W. These sizes agree with  
560 the commonly accepted notion that morphological units are scaled on the order of ~ 1-  
561 10 W but also demonstrate that they can be smaller than previously understood on the  
562 basis of the spacing concept alone.

563 Area percentages of the MU types ranged from 4.3 to 16.4%; however, five of the  
564 eight are within a couple of percentage points of each other. The Shannon diversity (Eq.  
565 1) for MUs on the LYR was 2.022 (as compared to a completely diverse value of 2.079).  
566 The evenness (Eq. 2) of polygon coverage was 0.973 (as compared to a fully even  
567 coverage value of 1.0), and the dominance (Eq. 3) value was 0.057 (as compared to a  
568 value of 0 for equal areas). The combination of these diversity indices shows no one  
569 particular MU type is dominating the segment area and that their population  
570 abundances are virtually equal, which is expected given the small range of abundance  
571 percentages. Whether MU equality constitutes MU randomness cannot be addressed  
572 with these metrics, so further testing was done.

573 This study utilizes a pixel size of 0.91 m x 0.91 m in ArcGIS to delineate MUs, which  
574 invariably resulted in some cases of a single pixel being characterized as an MU type  
575 and not adjacent other pixels of the same type (not considering diagonal pixels as  
576 adjacent). The area histograms (Fig. 7) show that this is true for all MU types. However,  
577 this small size could be considered more a discrete 'hydraulic unit' consisting of a highly  
578 localized landform at the next scale down of ~ 0.01-0.1 W. For most analyses, an MU  
579 landform should be readily identifiable in the field (e.g., Bisson et al., 1996). Because  
580 MUs are discretized using assessments of depth and velocity combinations derived  
581 from a 2D model at the 0.91 m x 0.91 m scale, an individual pixel whose depth and  
582 velocity combination forms a separate MU classification than all of its surrounding pixels  
583 could be considered either a real hydraulic unit or a model artifact caused by  
584 topographic noise (i.e., uncertainty at the meter scale) based on this delineation method  
585 rather than a fully realized MU landform. In fact, among all of the MU polygons, 45% are

586 only one pixel in size (varying from 32% to 49% for each MU type). The cumulative area  
587 of these one-pixel polygons, however, account for only 0.76% of the channel. An easy  
588 argument can be made, then, that eliminating these one-pixel polygons from  
589 geomorphic analyses involving areas would have negligible effects on the results.

590 Further analysis was conducted to explore how large a delineated polygon must be  
591 in order to consider it a real landform on the LYR. With every increase in a minimum  
592 size threshold in terms of numbers of pixels or planform area, more total area of the  
593 channel would also be eliminated from geomorphic analysis. For example, setting the  
594 minimum size threshold at 23.4 m<sup>2</sup> (28 pixels, or ~ 4.8 m x 4.8 m), the total number of  
595 polygons excluded would be 90.1% and the total area excluded would be 5.1%.

596 Increasing this threshold to 36.8 m<sup>2</sup> (44 pixels, or ~ 6.1 m x 6.1 m) yields an exclusion of  
597 92.3% of the number of polygons and 6.4% of the area. The minimum polygon size  
598 threshold that would retain at least 90% of the channel's area was thought to be  
599 meaningful and a good whole number, and that turned out to be a size of 92.8 m<sup>2</sup> (111  
600 pixels, or ~9.6 m x 9.6 m). This threshold would exclude 95% (another scientifically  
601 meaningful number) of the total number of polygons (Table 3); however, the high  
602 percentage of remaining area (90%) validates the concept that morphological units are  
603 on the commonly accepted scale of ~ 1-10 W in size and cover a majority of a channel's  
604 area. In addition to the minimum size of 92.8 m<sup>2</sup> retaining 90% of the channel area and  
605 excluding 95% of polygons for further analyses, this threshold size is also appropriately  
606 large enough for field surveyors to visually identify as a morphological landform (~ 1/6  
607 W), and is consistent with sizes used in other delineation methods (e.g., Bisson et al.,  
608 1996; Thomson et al., 2001). After applying this minimum size threshold, the mean unit

609 size for the remainder of each MU type ranged between  $\sim 0.4$ - $0.8$  W. Therefore, from a  
610 statistical and visual standpoint, the minimum size threshold for the following analyses  
611 for the LYR will be  $92.8 \text{ m}^2$ ; however, as a comparison the same analyses described  
612 hence will also be performed using no size discrimination. In the following analyses,  
613 when the minimum size discrimination is applied, the subthreshold areas become  
614 unclassified and therefore not used.

615

## 616 *6.2. Longitudinal distribution*

617 Chutes and runs were more predominant above DPD (Fig. 8A, F) and less abundant  
618 toward the mouth. Slackwater (Fig. 8G) and slow glide (Fig. 8H) units were distributed  
619 close to uniformly across the full segment. Pools (Fig. 8C) were unequally distributed  
620 between the upper and lower regions but mostly lacking in the middle, except for the  
621 large forced scour hole immediately downstream of the DPD spillway. Riffles exhibited  
622 near-uniform probabilities through most of the segment, except for the upper- and  
623 lowermost regions (Fig. 8D). Riffle transitions (Fig. 8E) and fast glides (Fig. 8B)  
624 exhibited their highest occurrence near the DPD, but are otherwise fairly uniform.  
625 Overall, chutes and pools exhibited the most extreme deviations from a uniform  
626 distribution.

627 The same distribution functions were calculated using only the minimum, field-  
628 identifiable polygon size as determined in the previous subsection. Omitting the 10% of  
629 area associated with the smallest polygons, however, did not noticeably affect the  
630 longitudinal distribution percentages. The mean of the differences in percentages of  
631 areas at each cross section was 0.58%, with the greatest differences occurring for the

632 slackwater (1.9%) and slow glide (1.2%) and the least for the run (0.02%) and chute  
633 (0.05%) distributions. These small differences did not affect the CDF slopes enough to  
634 alter the conclusions about the longitudinal distributions of each MU type along the  
635 channel. Therefore, the comparative distributions plots for the minimum size threshold  
636 are not presented here.

637

### 638 *6.3. Longitudinal spacing*

639 The longitudinal distribution results in section 6.2 show that some units, namely  
640 slackwater and slow glide, were so ubiquitous (i.e., near-uniform longitudinal  
641 distribution) and insufficiently longitudinally discrete for a test of spacing to be viable.  
642 Analysis of longitudinal spacing was therefore only performed for the six units that were  
643 distributed as longitudinally discrete units, i.e., chute, fast glide, pool, riffle, riffle  
644 transition, and run.

645 Histograms of the spacing lengths as expressed in terms of bankfull widths show  
646 unimodal distributions for each unit, with peaks between 2 and 3 W (Fig. 9). Mean  
647 spacings ranged from 2.7 to 4.4 W (runs and chutes are the respective end members).  
648 For direct comparisons with previous studies, the mean riffle and pool spacings were  
649 3.3 and 4.3 W, respectively, which is less than the commonly accepted values of 5-7 W,  
650 but within range of the  $\sim 3$  W reported by Carling and Orr (2000) for alluvial channels.  
651 For pool spacings, only  $\sim 29\%$  of the sequences exhibited distances of 5-7 W, and the  
652 mode was between 2 and 5 W ( $\sim 67\%$  of all spacings). For riffles,  $\sim 18\%$  of the  
653 spacings were between 5 and 7 W, with a mode of  $\sim 2-3$  W ( $\sim 46\%$ ). These results  
654 corroborate the hypothesis by Keller (1972) that longer sequences tend to be unstable

655 and break up into smaller spacings in nonideal conditions. Also of note is that riffles and  
656 pools exhibited different mean and mode spacings, which indicates that they are not  
657 necessarily linked together as a coupled unit.

658 For units that were not riffle or pool, little literature exists with which to compare our  
659 values. Chutes had a distinct mode at  $3 W$  and a mean of  $4.4 W$ , but were spaced as far  
660 as  $24 W$ . The fact that this has the largest mean may be because of its uneven  
661 distribution (Fig. 8), which shows that chutes are more abundant in the region just  
662 upstream of DPD. In fact, if DPD is used to separate the river segment into two reaches,  
663 then the mean chute spacings are  $3.3 W$  and  $6.3 W$  for upstream and downstream of the  
664 dam, respectively. However, pools also exhibited a similarly uneven distribution, but the  
665 spacings upstream and downstream of DPD were not as different ( $4.2 W$  and  $4.5 W$ ,  
666 respectively). Three units (pool, run, riffle transition) exhibited mean spacings that align  
667 with the mode (Fig. 9), which indicates that their locations are more stable and their  
668 recurrences more regular.

669

#### 670 *6.4. Adjacency*

671 Adjacency results show that a strong organizational structure is evident (Table 4;  
672 Fig. 10). This could be an artifact of the classification metric; however, the metric was  
673 created with an eye to actual physical conditions, so this is likely a true representation of  
674 landform organization. A clear grouping of collocated steep, constricted units (i.e., riffle,  
675 run, and chute) emerged, whereas pools did not exhibit strong mutual collocations. Fast  
676 glide, riffle transition, and slow glide existed as buffers between the grouping of riffle–  
677 run–chute and the other unit types (Fig. 10A). Meanwhile, riffle→pool and pool→riffle

678 adjacencies had greater-than-random avoidance (Table 4), which differs from  
679 traditional, simplistic methods for identifying only pool and riffle MUs in a channel.

680 The results in Table 4 include all MU polygons, regardless of size. To evaluate  
681 whether adopting the field-identifiable minimum size threshold affects these results, the  
682 same analysis was performed for just those MU polygons with areas  $> 92.8 \text{ m}^2$  (Table  
683 5). The total number of adjacencies in the segment corridor is reduced to  $\sim 2.5\%$  of the  
684 raw count. Most connections that were considered as scientifically significant  
685 collocations remained so (Fig. 10B). The two exceptions were riffle  $\rightarrow$  slow glide and riffle  
686 transition  $\rightarrow$  slackwater, which changed to avoidance and near-random, respectively.  
687 Two of the three previously near-random adjacencies changed to collocation  
688 (pool  $\rightarrow$  slackwater and riffle  $\rightarrow$  run), while the third changed to avoidance  
689 (riffle  $\rightarrow$  slackwater). Six previous avoidance probabilities changed to greater-than-  
690 random collocation: riffle  $\rightarrow$  chute; fast glide  $\rightarrow$  run; riffle transition  $\rightarrow$  fast glide; riffle  
691 transition  $\rightarrow$  riffle; slackwater  $\rightarrow$  pool; and slow glide  $\rightarrow$  fast glide. Eight other adjacent  
692 combinations also increased from avoidance to near-random (Table 5).

693

#### 694 *6.5. Lateral variability*

695 Considering that the mean MU sizes are  $< 1.0 W$  (section 6.1), we should expect  
696 laterally coherent MUs. Employing no minimum size discrimination of the MU polygons,  
697 the LYR exhibited an average of  $\sim 18$  units per base-flow width (Fig. 11A). If the margin  
698 units are pixilated and separated from one cohesive unit into 5 or 6 diagonally adjacent  
699 units, then this number can be justified. In fact, on average  $\sim 57\%$  of the polygons at  
700 each cross section were comprised of slackwater and slow glide units at this scale.



701 However, most field observers would likely have a difficult time visualizing that many  
702 units across an ~ 60-m channel (e.g., about one unit every 3 m). Applying the minimum  
703 field-identifiable MU size threshold, the average number of units per cross section  
704 decreases to a value of six (Fig. 11B). An example of how six MUs might occur across  
705 one cross section would be if there were slackwater and slow glide units along both  
706 banks bookending a mid-channel fast glide and pool (Fig. 4). The implication of this  
707 analysis is that any given cross section is not necessarily associated with any one MU,  
708 as is typically assumed and reported. Therefore each cross section does not exhibit any  
709 one combination of hydraulics and, therefore, not any one potential habitat. Instead, a  
710 complex and diverse suite of landforms and potential habitat exist at any given cross  
711 section in a gravel–cobble river. Capturing this spatial complexity is where 2D planview  
712 MU analysis has the most value. The statistical analyses herein reduce that complexity  
713 to scientifically meaningful metrics.

#### 715 *6.6. Hydromorphic characteristics*

716 The lateral variability results show that each cross section was comprised of more  
717 than one MU. However, ~ 25% of the cross sections in the LYR were comprised of an  
718 MU that made up at least 60% of the area in the cross-sectional rectangle. Therefore,  
719 those cross sections were considered to contain a 'dominant' MU for the following  
720 analyses, and only those MU-dominated cross sections were analyzed for their relative  
721 hydromorphic characteristics.

722 The wetted width of representative cross sections also varied significantly by MU.  
723 Slackwater and riffle transition units tend to occur in wide channel sections (Table 6),

724 while chutes and runs occur in narrower ones. MU-averaged widths were highly  
725 statistically different ( $p < 0.01$ ) for 24 out of 28 MU pairs. The other four MU pairs that  
726 were statistically indifferent at the 95% confidence level involved slow glide (versus  
727 pool, riffle, and riffle transition), while the other one was between fast glide and riffle.

728 Cross sections dominated by riffles exhibit the highest WSS (Table 6), almost double  
729 that of the next highest (chute). Pools and slackwater cross sections exhibit the lowest  
730 mean slopes. Using a Mann-Whitney rank sum U test, mean slopes of 24 out of 28 pairs  
731 of MU types were highly statistically different ( $p < 0.01$ ). Fast glide and slow glide were  
732 significantly different at the 95% confidence level ( $p < 0.05$ ). The exceptions where  
733 mean slopes were statistically indistinct ( $p > 0.05$ ) included riffle transition–run, fast  
734 glide–slackwater, and slow glide–slackwater.

735 The channel cross sections dominated by each MU type exhibited a very high  
736 bankfull width–depth ratio (i.e.,  $> 40$ ), except for pool (Table 6). Pool-dominated cross  
737 sections were also the only ones that exhibited any width–depth ratios  $< 12$ , and in fact,  
738 only 8.2% of the pool sections exhibited values  $> 40$ . Amongst the other MU types, a  
739 majority of their dominated cross sections exhibited width–depth ratios  $> 40$  (ranging  
740 from  $\sim 75$  to 100%). Only chute-dominated cross sections were all  $> 40$  (Table 6).

741 Using a Mann-Whitney rank sum U test, mean width–depth ratios of 15 out of 28  
742 pairs of MU types were highly statistically different ( $p < 0.01$ ). Chute was significantly  
743 different ( $p < 0.05$ ) from riffle transition and slow glide. Notably, pool was the only unit to  
744 exhibit high statistical significance from all the other MU types. The MU pairs that were  
745 statistically indifferent include: chute–riffle, chute–slackwater, fast glide–run, fast glide–

746 slackwater, fast glide–slow glide, riffle–slackwater, riffle transition–slackwater, riffle  
747 transition–slow glide, run–slackwater, run–slow glide, and slackwater–slow glide.

748

## 749 **7. Discussion**

750 Channel morphology is shaped by several complex and interrelated processes, such  
751 as upstream hydrology, transport capabilities of the substrate, channel–floodplain  
752 interactions, and flow hydraulics. While some inherent randomness might exist in these  
753 processes, the resulting morphological patterns are nonrandom and nonuniform, as  
754 exemplified by the analyses discussed herein. Each MU type exhibited some particular  
755 spatial organization characteristics within the LYR. The following subsections provide  
756 some context for interpreting these results.

757

### 758 *7.1. Effect of imposing a minimum size for MUs*

759 Previous field delineation procedures have typically set a minimum size for MUs  
760 subject to the user's ability to discern contiguous properties at a particular scale (e.g.,  
761 Bisson et al., 1996). For the methodology used herein, the MUs are digitally delineated  
762 using a 0.91 m x 0.91 m pixel scale. However, it is suggested that an MU of this size is  
763 difficult to field-verify and does not constitute a reasonably discrete landform free of data  
764 collection noise. Therefore, a size of 92.8 m<sup>2</sup> was decided as a minimum scale for units  
765 in the LYR on the basis that it constituted the 90<sup>th</sup> percentile of polygon size. Spatial  
766 analyses were performed on the MUs using the raw and the thresholded sets of  
767 polygons, which thus introduces the question of whether this size discrimination affected  
768 the results and their associated interpretations.

769 Polygon segregation had the largest impact among analyses for slackwater and slow  
770 glide as they experienced the largest reductions in number of polygons and in total  
771 channel area (Table 3). The problem is that these are the long, skinny units that require  
772 a finer resolution than ~ 1 m to obtain multiple contiguous pixels forming coherent MU  
773 polygons of ~ 5 m width, given the overall width of the LYR. The order of MUs from  
774 largest to smallest in total area, excluding slackwater and slow glide, is the same  
775 irrespective of the minimum size application. However, an analysis including all  
776 polygons would show that slackwater is the most abundant, whereas pool covers the  
777 most area if only the field-identifiable sizes are used. Ignoring the areas that are  
778 comprised of a complex array of small units could have an impact on river management  
779 schemes, even if it is only 10% of the channel.

780 The interpretations of the longitudinal analyses for each unit do not change with  
781 minimum size segregation. This suggests that large polygons of any particular MU tend  
782 to be spatially associated with smaller polygons of the same type. Ignoring the smaller  
783 polygons, therefore, does not lead to ignoring whole areas where an MU is identifiably  
784 abundant.

785 For the adjacency analyses, the size segregation affects the large ↔ small polygon  
786 transitions. Removing the small polygons reduced the number of adjacencies by ~  
787 97.5%, which suggests that many large polygons were ringed by smaller, noncohesive  
788 units. The most significant impact is that the riffle → slow glide transition switched from  
789 statistically collocated to avoided. Conversely, a couple of adjacencies switched from  
790 avoidance to collocation using only the larger polygons, namely riffle → chute and  
791 slackwater → pool. Several other adjacencies switched from being statistically avoided

792 to near-random (Tables 4 and 5). For the most part, the other adjacency distinctions  
793 remained the same.

794 The most extreme difference in results using the minimum size polygons is that for  
795 counting the number of MUs laterally across the channel. Using all polygons, the  
796 average number of MUs per cross section is almost 20, but that number reduces to  
797 about six if the smaller polygons are excluded. This difference, however, does not  
798 change the interpretation that large gravel–cobble rivers exhibit significant lateral  
799 variability in channel morphology, which has been neglected in the past but should now  
800 be accounted for in river science and management. Even with this size discrimination,  
801 every cross section exhibits more than one MU across its width. The ability to recognize  
802 this amount of lateral variability represents a shift in the manner in which river scientists  
803 have usually mapped channels.

804 In summary, using a minimum size threshold changes some of the details but not  
805 the overall results that MUs in a cobble-bed river exhibit a deterministic organizational  
806 pattern.

## 808 *7.2. Base flow versus bankfull flow as a normalizing discharge*

809 A decision was made for this study to use mean bankfull wetted width as the  
810 normalizing variable for longitudinal spacing analyses. An alternative would be to  
811 normalize by mean base-flow channel width, because that is the relevant discharge at  
812 which the MUs were identified and delineated. Other studies of unit spacings have also  
813 typically used the discharge at observation, which tends to be somewhere between  
814 base flow and bankfull and is usually called ‘active channel width’ (e.g., Grant et al.,

815 1990). The question of which mean width to use depends on several factors. First, a  
816 single bankfull discharge may or may not be identifiable or appropriate for a given river,  
817 as a function of landscape context, disturbance regimes, and/or climate and climatic  
818 change. Second, as the lengths of study segments that can be accurately interpreted  
819 with 2D models increase, the hydrology within these study segments may be gaining or  
820 losing too much water to rely on a single discharge metric. This study spanned ~ 37 km  
821 of channel but was in a lowland context with no sizable unregulated tributaries. Third,  
822 the appropriate width to use may also hinge on whether the controlling hydraulics that  
823 influence MU organization occur during base flow, bankfull, or some other significantly  
824 larger discharge.

825 This decision, however, may influence the values calculated for the MUs in the LYR  
826 and, hence, comparisons to other systems. For comparison, therefore, the averaged  
827 longitudinal spacings for each MU were also normalized by mean base-flow width as a  
828 sensitivity test. The mean bankfull width for the LYR is 97.3 m, the mean base-flow  
829 width is 59.5 m (about 40% narrower), and the spacings are each altered by about this  
830 same amount (Table 7). Interestingly, the distances between successive units now  
831 become more comparable to previously published values of 5-7 W. Riffle spacings  
832 would be 5.4 W, and pools 7.0 W. The spacings for the other units also increase to  
833 within or near the 5-7 W range; however, without other studies with which to compare,  
834 what their expected values should be is difficult to know. Overall, insufficient data exist  
835 to set a standard at this time, so practitioners are recommended to use their judgment  
836 based on conditions in their study segment and be transparent in reporting their chosen  
837 discharge.

838

839 *7.3. Syntheses of spatial patterns for each MU*

840 By synthesizing the results by MU, a unique picture emerges for the observed  
841 pattern and organization of each unit within the LYR (Table 8). Above all else, this study  
842 found that the euphemism of a 'riffle–pool unit' certainly would be invalid for the LYR  
843 and likely for other rivers once analyzed in higher resolution using 2D MUs. Several of  
844 the spatial analyses presented herein highlight the lack of coupling between these units.  
845 First, pools occur in greater abundance than riffles in terms of planform area. Using the  
846 minimum size discrimination, pools are the most abundant unit while riffles are the fifth  
847 most (Table 3). Second, pools are spaced apart ~ 1-2 W more than riffles on average  
848 (Fig. 9). Third, pools and riffles are not spatially collocated to each other (Fig. 10). When  
849 viewed as laterally discrete landforms, riffles tend to group with chute and run. Because  
850 these three MU types have significantly different base-flow depths, the interpretation is  
851 that their common high velocities must be because of high slopes and/or local  
852 constrictions, which would be vertical for riffles and lateral for runs and chutes.  
853 Meanwhile, pools do not exist in a clear grouping, but show one-way adjacencies to fast  
854 and slow glides and a weaker bidirectional collocation with slackwater. The common  
855 term 'riffle–pool unit', therefore, should be reinterpreted reflecting its low resolution,  
856 reach-scale perspective to actually mean 'a hole in part of the riverbed surrounded and  
857 followed by flatter areas and eventually transitioning to a steep, constricted region'.  
858 Because longitudinal profiles often arbitrarily follow the thalweg as opposed to the  
859 centerline or other streamline, they go through pools disproportionate to their actual  
860 areal presence (Table 2), giving pools more weight than they are possibly due.

861 Therefore, an important future direction should be explaining why large swaths of a  
862 channel are relatively flat compared to past work explaining why there exists holes and  
863 bumps in a thalweg profile, which are preferentially selected to capture those holes and  
864 bumps.

865 Looking beyond the narrow view of MU types dominated by riffles and pools, this  
866 study found interesting patterns for other unit types as well. Chutes, for example,  
867 occupied the smallest area of the LYR segment; tended to cluster upstream of DPD and  
868 avoided the mouth; exhibited the longest average spacing of about 4.4 W from each  
869 other; were preferentially adjacent to runs and riffles; and were laterally associated with  
870 less than five other MUs per cross section. The next most abundant units were runs that  
871 tended to cluster upstream of DPD and also avoided the mouth; exhibited the shortest  
872 average spacing of about 2.7 W from each other; were preferentially adjacent to fast  
873 glide, riffle, and riffle transition; and were laterally associated with over five other MUs  
874 per cross section. Slackwaters and slow glides were both near-uniformly distributed  
875 along the channel hugging the margin, with some slight clustering in the downstream  
876 regions; both exhibited adjacency collocations to each other and to riffle transitions;  
877 however slackwater tended to be laterally associated with fewer other MUs per cross  
878 section than slow glide. Fast glides and riffle transitions occupied about the same  
879 percentage of the segment area and had similar longitudinal spacing values, but  
880 differed in their preferential locations along the LYR: where fast glides tended to avoid  
881 the upstream bedrock regions and clustered around the DPD, and riffle transitions  
882 tended to avoid the mouth but were otherwise prevalent downstream of DPD.

883



884 *7.4. Deterministic characteristics of MU patterns*

885 The hydromorphic characteristics provide a synthesis of the channel morphology at  
886 locations in which a majority of the base-flow wetted width was dominated by a  
887 particular MU (Table 6). For example, pools tended to be located in deep areas with low  
888 water surface slopes. Riffles tended to occur in wide areas with high water surface  
889 slopes. Slackwater areas exhibited the highest base-flow wetted widths and high values  
890 of width–depth ratios. This signifies that slackwater units occurred in regions in which  
891 the valley base is very wide and flat, i.e., without a well-defined channel.

892 An important conclusion from this study is that MU patterns are nonrandom. The  
893 next logical question should then be, why? If a particular unit tends to cluster in or  
894 similarly avoid a certain region of the river, are there characteristics of the river valley  
895 that cause these patterns? Does this result then suggest that the patterns are therefore  
896 deterministic, i.e., qualitatively predictable? The mechanistic origins of these units are  
897 still poorly understood, but it was previously demonstrated that flow convergence  
898 routing was existent in at least one pool–riffle–run sequence on the LYR (Sawyer et al.,  
899 2010); and consistent with that mechanism, the longitudinal positioning of riffle crests in  
900 Timbuctoo Bend (Fig. 1) has persisted for decades (White et al., 2010). A full  
901 understanding of such mechanisms is beyond the scope of this study, but a strong case  
902 can be made that any such mechanism that is dependent on multiscale landscape  
903 heterogeneity will require a spatially explicit and sufficiently objective method for  
904 characterizing landforms, such as the approach demonstrated in this study.

905

906 *7.5. Future directions*

907 Once an accurate map of the landforms has been established, it can be used to  
908 stratify biologic and stage-dependent hydraulic data sets and as a baseline for future  
909 geomorphic change analyses. The LYR MU map has previously been incorporated into  
910 studies of the riparian vegetation (Abu-Aly et al., 2013) and spawning habitat suitability  
911 for Chinook salmon (Pasternack et al., 2013). Any comprehensive landform map can  
912 serve as the basis for a 'bottom-up' approach to understanding and linking the channel  
913 morphology with the ecologic habitat and can guide river management and rehabilitation  
914 strategies.

915 For this study, the MUs were mapped and analyzed only within the base-flow region  
916 of the LYR. However, rivers are more than just their base-flow channels; and if the  
917 spatial scope were to increase outward to the valley walls, other landform types would  
918 become included, such as bars, swales, and floodplains, etc. The purpose of this study  
919 was to highlight the inherent spatial organization of in-channel landforms, and the same  
920 analyses reported here could translate to a broader study that includes bankfull and out-  
921 of-channel MUs. Wyrick and Pasternack (2012) extended the in-channel methods and  
922 concept presented herein to the entire river corridor, but the full scope of that analysis is  
923 beyond what could be presented at this time.

924

925 **8. Conclusions**

926 The MUs represent distinct form–process associations and are important links in  
927 hierarchical morphology frameworks. Gravel–cobble rivers exhibit a high diversity of  
928 landforms; however, each MU type differs in streamwise distribution and spacing,

929 adjacency collocations and avoidances, and lateral variability. Each MU type tends to  
930 preferentially occur within regions of distinct valley and channel characteristics.

931       Because of the near-census approach to surveying and modeling our study site, the  
932 results of the digital delineation and subsequent spatial analyses are scaled to sizes  
933 much smaller than what field methods produce, therefore creating maps that are more  
934 detailed and ultimately more accurate than large-scale averaging. Thus, this study  
935 highlights several key advances to the science and analysis of river morphology  
936 organization, some of which may seem to confute traditional knowledge but are a result  
937 of this increased resolution. First, a diverse suite of MU types that can comprise a river  
938 channel exist, not just pools and riffles. This point is particularly important for  
939 recognizing the inherent complexity of a channel's morphology and the relative role that  
940 plays in management strategies. Second, because the traditional pool–riffle morphology  
941 has persisted throughout the literature, spatial organization analyses of other MU types  
942 are lacking. Therefore, this study starts the discussion on the geospatial context for  
943 other MUs, such as runs, glides, and chutes. Third, all of the MU types exhibit a  
944 nonrandom spatial organization, indicating a natural structure to the channel  
945 morphology of a gravel–cobble river. Fourth, a cross section is often not defined by a  
946 single MU type. The discovery of laterally explicit MU variation represents an important  
947 link to the ecologic function of rivers. Fifth, the MU map is robust enough that the  
948 interpretation of the spatial organization does not significantly change by imposing a  
949 minimum size threshold on the delineated polygons to be used in the analyses.

950

951 **Acknowledgements**

952 Funding for this study was provided by the Yuba County Water Agency. Extensive  
953 knowledge and experience of the LYR that helped finalize the MU thresholds, and maps  
954 were provided by a consortium of experts that make up the Yuba River Accord  
955 Management Team (more information available at [www.yubaaccordrmt.com](http://www.yubaaccordrmt.com)).

956

957 **References**

- 958 Abu-Aly, T.R., Pasternack, G.B., Wyrick, J.R., Barker, R., Massa, D., Johnson, T., 2013.  
959 Effects of LiDAR-derived, spatially-distributed vegetative roughness on 2D  
960 hydraulics in a gravel-cobble river at flows of 0.2 to 20 times bankfull.  
961 Geomorphology, <http://dx.doi.org/10.1016/j.geomorph.2013.10.017>.
- 962 Barker, J.R., 2011. Rapid, abundant velocity observation to validate million-element 2D  
963 hydrodynamic models. M.S. Thesis, University of California at Davis, Davis, CA.
- 964 Bisson, P.A., Montgomery, D.R., Buffington, J.M., 1996. Valley segments, stream  
965 reaches, and channel units. In: Hauer, F.R., Lambert, G.A. (Eds.), *Methods in*  
966 *Stream Ecology*. Academic Press, San Diego, CA, USA, pp. 23-52.
- 967 Borsanyi, P., Alfredson, K., Harby, A., Ugedal, O., Kraxner, C., 2004. A meso-scale  
968 habitat classification method for production modeling of Atlantic salmon in Norway.  
969 *Hydroécologie Appliquée* 14 (1), 119-138.
- 970 Carley, J.K., Pasternack, G.B., Wyrick, J.R., Barker, J.R., Bratovich, P.M., Massa, D.A.,  
971 Reedy, G.D., Johnson, T.R., 2012. Significant decadal channel change 58–67 years  
972 post-dam accounting for uncertainty in topographic change detection between  
973 contour maps and point cloud models. *Geomorphology*,  
974 [doi:10.1016/j.geomorph.2012.08.001](https://doi.org/10.1016/j.geomorph.2012.08.001).

975 Carling, P.A., Orr, H.G., 2000. Morphology of riffle-pool sequences in the river Severn,  
976 England. *Earth Surface Processes and Landforms* 25, 369-384.

977 Frissell, C.A., Liss, W.J., Warren, C.E., Hurley, M.D., 1986. A hierarchical framework for  
978 stream habitat classification: viewing streams in a watershed context. *Environmental*  
979 *Management* 10 (2), 199-214.

980 Grant, G.E., Swanson, F.J., Wolman, M.G., 1990. Pattern and origin of stepped-bed  
981 morphology in high-gradient streams, western Cascades, Oregon. *Geological*  
982 *Society of America Bulletin* 102, 340-352.

983 Gray, M., 2004. *Geodiversity: Valuing and Conserving Abiotic Habitats*. Wiley,  
984 Chichester, UK.

985 Gregory, K.J., Gurnell, A.M., Hill, C.T., Tooth, S., 1994. Stability of the pool-riffle  
986 sequence in changing river channels. *Regulated Rivers: Resources Management* 9,  
987 35-43.

988 Halwas, K.L., Church, M., 2002. Channel units in small, high gradient streams on  
989 Vancouver Island, British Columbia. *Geomorphology* 43, 243-256.

990 Hauer, C., Mandlbürger, G., Habersack, H., 2009. Hydraulically related hydro-  
991 morphological units: description based on a new conceptual mesohabitat evaluation  
992 model (MEM) using LiDAR data as geometric input. *River Research and*  
993 *Applications* 25, 29-47.

994 Hawkins, C.P., Kershner, J.L., Bisson, P.A., Bryant, M.D., Decker, L.M., Gregory, S.V.,  
995 McCullough, D.A., Overton, C.K., Reeves, G.H., Steedman, R.J., Young, M.K.,  
996 1993. A hierarchical approach to classifying habitats in small streams. *Fisheries*  
997 18(6), 3-12.

998 James, L.A., Singer, M.B., Ghoshal, S., Megison, M., 2009. Historical channel changes  
999 in the lower Yuba and Feather Rivers, California: long-term effects of contrasting  
1000 river-management strategies, In: James, L.A., Rathburn, S.L., Whittecar, G.R.  
1001 (Eds.), Management and Restoration of Fluvial Systems with Broad Historical  
1002 Changes and Human Impacts. Geological Society of America Special Paper 451,  
1003 pp. 57-81, doi: 10.1130/2008.2451(04).

1004 Keller, E.A., 1972. Development of alluvial stream channels: a five-stage model.  
1005 Geological Society of America Bulletin 83 (5), 1531-1536.

1006 Keller, E.A., Melhorn, W.N., 1978. Rhythmic spacing and origin of pools and riffles.  
1007 Geological Society of America Bulletin 89 (5), 723-730.

1008 Klaar, M.J., Maddock, I., Milner, A.M., 2009. The development of hydraulic and  
1009 geomorphic complexity in recently formed streams in Glacier Bay National Park,  
1010 Alaska. River Research and Applications 25, 1331-1338.

1011 Knighton, D., 1998. Fluvial Forms and Processes: A New Perspective. Edward Arnold  
1012 Publishers Ltd, London, UK.

1013 Lai, Y.G., 2008. SRH-2D version 2: Theory and User's Manual. U.S. Department of the  
1014 Interior, Bureau of Reclamation, Technical Service Center, Denver, CO.

1015 Leopold, L.B., Wolman, G.M., Miller, J.P., 1964. Fluvial Processes in Geomorphology.  
1016 W.F. Freeman and Company, San Francisco, CA, USA.

1017 Maddock, I., 1999. The importance of physical habitat assessment for evaluating river  
1018 health. Freshwater Biology 41, 373-391.

1019 Maddock, I., Smolar-Zvanut, N., Hill, G., 2008. The effect of flow regulation on the  
1020 distribution and dynamics of channel geomorphic units (CGUs) and implications for

1021 Marble Trout (*Salmo marmoratus*) spawning habitat in the Soča River, Slovenia. IOP  
1022 Conference Series: Earth and Environmental Science 4, 1-10.

1023 Madej, M.A., 2001. Development of channel organization and roughness following  
1024 sediment pulses in single-thread, gravel bed rivers. Water Resources Research 37  
1025 (8), 2259-2272.

1026 Milan, D.J., Heritage, G.L., Large, A.R.G., Entwistle, N.S., 2010. Mapping hydraulic  
1027 biotopes using terrestrial laser scan data of water surface properties. Earth Surface  
1028 Processes and Landforms 35, 918-931.

1029 Moir, H.J., Pasternack, G.B., 2008. Relationships between mesoscale morphological  
1030 units, stream hydraulics and Chinook salmon (*Oncorhynchus tshawytscha*)  
1031 spawning habitat on the lower Yuba River, California. Geomorphology 100, 527-548.

1032 Moir, H.J., Pasternack, G.B., 2010. Substrate requirements for spawning Chinook  
1033 salmon (*Oncorhynchus Tshawytscha*) are dependent on local channel hydraulics.  
1034 River Research and Applications 26, 456-468.

1035 Montgomery, D.R., Buffington, J.M., Smith, R.D., Schmidt, K.M., Pess, G., 1995. Pool  
1036 spacing in forest channels. Water Resources Research 31 (4), 1097-1105.

1037 Newson, M.D., Large, A.R.G., 2006. 'Natural' rivers, 'hydromorphological quality' and  
1038 river restoration: a challenging new agenda for applied fluvial geomorphology. Earth  
1039 Surface Processes and Landforms 31, 1606-1624.

1040 Newson, M.D., Newson, C.L., 2000. Geomorphology, ecology and river channel habitat:  
1041 mesoscale approaches to basin-scale challenges. Progress in Physical Geography  
1042 24 (2), 195-217.

1043 O'Neill, M.P., Abrahams, A.D., 1984. Objective identification of pools and riffles. Water  
1044 Resources Research 20 (7), 921-926.

1045 Parker, G., 1976. On the cause and characteristic scales of meandering and braiding in  
1046 rivers. Journal of Fluid Mechanics 76 (3), 457-480.

1047 Pasternack, G.B., 2008. SHIRA-Based River Analysis and Field-Based Manipulative  
1048 Sediment Transport Experiments to Balance Habitat and Geomorphic Goals on the  
1049 Lower Yuba River. Cooperative Ecosystems Studies Unit (CESU) 81332 6 J002  
1050 Final Report, University of California at Davis, Davis, CA, 569 pp.

1051 Pasternack, G.B., 2009. Specific Sampling Protocols and Procedures for Topographic  
1052 Mapping. The Lower Yuba River Accord Planning Team, Marysville, CA.

1053 Pasternack, G.B., 2011. 2D Modeling and Ecohydraulic Analysis. Createspace, Seattle,  
1054 WA.

1055 Pasternack, G.B., Tu, D., Wyrick, J.R., 2013. Chinook adult salmon spawning physical  
1056 habitat of the lower Yuba River. Prepared for The Lower Yuba River Accord River  
1057 Management Team, University of California, Davis, CA. Available at  
1058 [www.yubaaccordrmt.com](http://www.yubaaccordrmt.com).

1059 Reid, H.E., Gregory, C.E., Brierley, G.J., 2008. Measures of physical heterogeneity in  
1060 appraisal of geomorphic river condition for urban streams: Twin Streams catchment,  
1061 Auckland, New Zealand. Physical Geography 29 (3), 247-274.

1062 Richards, K.S., 1976. The morphology of riffle-pool sequences. Earth Surface  
1063 Processes and Landforms 1, 71-88.

1064 Rosgen, D., 1996. Applied River Morphology. Wildland Hydrology, Pagosa Springs, CO,  
1065 USA.



1066 Sawyer, A.M., Pasternack, G.B., Moir, H.J., Fulton, A.A., 2010. Riffle-pool maintenance  
1067 and flow convergence routing observed on a large gravel-bed river. *Geomorphology*  
1068 114, 143-160.

1069 Schwartz, J.S., Herricks, E.E., 2008. Fish use of ecohydraulic-based mesohabitat units  
1070 in a low gradient Illinois stream: implications for stream restoration. *Aquatic*  
1071 *Conservation: Marine and Freshwater Ecosystems* 18, 852-866.

1072 Thompson, A., 1986. Secondary flows and the pool-riffle unit: a case study of the  
1073 processes of meander development. *Earth Surface Processes and Landforms* 11  
1074 (6), 631-641.

1075 Thomson, J.R., Taylor, M.P., Fryirs, K.A., Brierley, G.J., 2001. A geomorphological  
1076 framework for river characterization and habitat assessment. *Aquatic Conservation-*  
1077 *Marine and Freshwater Ecosystems* 11 (5), 373-389.

1078 Wadeson, R.A., 1994. A geomorphological approach to the identification and  
1079 classification of instream flow environments. *Southern African Journal of Aquatic*  
1080 *Sciences* 20, 38-61.

1081 Wadeson, R.A., Rowntree, K.M., 1998. Application of the hydraulic biotope concept to  
1082 the classification of instream habitats. *Aquatic Ecosystems Health and Management*  
1083 1, 143-157.

1084 White, J.Q., Pasternack, G.B., Moir, H.J., 2010. Valley width variation influences riffle-  
1085 pool location and persistence on a rapidly incising gravel-bed river. *Geomorphology*  
1086 121, 206-221.

1087 Wyrick, J.R., Pasternack, G.B., 2012. Landforms of the Lower Yuba River. Prepared for  
1088 the Yuba Accord River Management Team, University of California, Davis. Available  
1089 at [www.yubaaccordrmt.com](http://www.yubaaccordrmt.com).

1090 Zimmer, M.P., Power, M., 2006. Brown trout spawning habitat preferences and redd  
1091 characteristics in the Credit River, Ontario. Journal of Fish Biology 68, 1333-1346.

1092

Uncorrected Final Manuscript

1093 Figure Titles

1094

1095 Fig. 1. Location map of the Lower Yuba River (LYR).

1096

1097 Fig. 2. Flowchart of MU delineation procedure. Parallelograms represent prepared data  
1098 input; trapezoids represent manual input; diamonds represent decisions.

1099

1100 Fig. 3. Hydraulic thresholds for delineating MUs within the LYR at the selected base  
1101 flow discharge.

1102

1103 Fig. 4. A sample location of the LYR's MU map that includes the cross-sectional boxes  
1104 used for the longitudinal distribution and lateral variability analyses.

1105

1106 Fig. 5. A sample MU sequence that illustrates an example of an MU type (riffle  
1107 transition) being located as two separate polygons on opposite sides of the channel  
1108 from each other. For the longitudinal spacing analyses, this duad was combined into  
1109 one unit. The black line represents the base-flow thalweg.

1110

1111 Fig. 6. A theoretical schematic of lateral MU variability within a channel. For the  
1112 adjacency analyses, unit A would exhibit three transitions to unit B; however, the three  
1113 units B all touch the same unit A and would therefore only count as one transition.

1114

1115 Fig. 7. Histograms of the individual polygon areas delineated for each MU type. The  
1116 dashed line represents the cumulative percent area.

1117

1118 Fig. 8. Longitudinal distributions for each MU type based on percent of total area within  
1119 each cross-sectional box (e.g., Fig. 4). The gray lines represent the discrete  
1120 percentages of areas for each cross section. The dark black line represents the  
1121 cumulative percentages of areas as measured from the mouth to the top of the  
1122 segment. The diagonal lines represent a theoretical uniform cumulative distribution.

1123

1124 Fig. 9. Histograms of the sequential streamwise distances between like units. The  
1125 absolute distances were normalized by the mean channel bankfull width. Any spacings  
1126 in the '15' column actually represent spacings of '15 or more' channel widths.

1127

1128 Fig. 10. Collocation adjacency diagrams between MUs using (A) all delineated  
1129 polygons, and (B) only the polygons larger than the minimum size threshold. For a full  
1130 summary of adjacencies, refer to Tables 3 and 4.

1131

1132 Fig. 11. Total number of MU polygons within each cross-sectional box (e.g., Fig. 4)  
1133 using (A) all delineated polygons, and (B) only the polygons larger than the minimum  
1134 size threshold. The dark lines represent the segment averages.

1135

Table 1

Descriptions of morphological units that occur within the LYR

Morphological unit	Description at base flow
pool	Topographic low in the channel that exhibits high depth and low velocity, and low water surface slope. This unit covers 'forced pool' and 'pool'. A forced pool is one that is typically along the periphery of the channel and is 'over-deepened' from local convective acceleration and scour during floods that is often associated with static structures such as wood, boulders, and bedrock outcrops. A pool is not formed by a forcing obstruction. The distinction between forced pool and pool cannot be made automatically within GIS.
riffle	An area with shallow depths, moderate to high velocities, rough water surface texture, and steep water surface slope. Riffles are generally associated with the crest and backslope of a transverse bar (e.g., Knighton, 1998).
run	An area with moderate velocity, high depths, and moderate water surface slope. Runs typically occur in straight sections that exhibit a moderate water surface texture and tend not to be located over transverse bars.
chute	An area of high velocity, steep water surface slope, and moderate to high depth located in the channel thalweg. Chutes are often located at an abrupt vertical expansion.
fast glide	An area of moderate velocity and depth and low water surface slope. Fast glides commonly occur along the periphery of channels and flanking pools. Fast glides can also exist in straight sections of low bed slope.
slow glide	An area of low velocity, low to moderate depths, and low water surface slope. Slow glides may be located near water's edge as other MUs along the channel thalweg transitions laterally towards the stream margins.
slackwater	A shallow, low velocity region of the stream that is typically located within adjacent embayments, side channels, or along channel margins. Velocities are near stagnant during base flow conditions and rise more slowly than in other units as stage increases.
riffle transition	Typically a transitional area between an upstream MU into a riffle or from a riffle into a downstream MU. Water depth is relatively low. Velocity is also relatively low, but increases downstream due to convective acceleration toward a shallow riffle crest that is caused by lateral and vertical flow convergence. The upstream limit is at the approximate location where there is a transition from a divergent to convergent flow pattern. The downstream limit is at the slope break of the channel bed termed the 'riffle crest'.

Table 2  
Area and size statistics of morphological units

Morphological unit	Total area (ha)	Number (-)	Maximum (m <sup>2</sup> )	Median (m <sup>2</sup> )	Mean (m <sup>2</sup> )	Polygon size threshold for 90% of total MU area (m <sup>2</sup> )
chute	8.86	606	7,220	4.2	146	185
fast glide	29.4	2,919	19,394	1.7	101	195
pool	32.9	814	71,746	2.5	404	936
riffle	27.2	1,988	8,998	2.5	137	268
riffle transition	31.7	6,604	28,060	1.7	48.1	78.6
run	17.9	1,455	7,784	1.7	123	204
slackwater	33.8	13,686	18,600	1.7	24.8	24.2
slow glide	24.7	12,981	12,598	1.7	19.1	14.2
All units	206.5	41,053	71,746	1.7	50.5	92.8

Table 3

Area and number of polygons delineated as each corresponding MU type for abundance analyses that include all mapped polygons (left side) and only those polygons larger than a field-identifiable size of 92.8 m<sup>2</sup> (right side)

Morphological unit	All MU polygons				Only MUs larger than minimum threshold			
	Area (ha)	Area (%)	Number (-)	Number (%)	Area (ha)	Area (%)	Number (-)	Number (%)
chute	8.86	4.3	606	1.5	8.33	4.5	116	6.0
fast glide	29.4	14.2	2,919	7.1	27.3	14.7	214	11.0
pool	32.9	15.9	814	2.0	32.3	17.4	134	6.9
riffle	27.2	13.2	1,988	4.8	25.9	13.9	228	11.7
riffle transition	31.7	15.4	6,604	16.1	28.2	15.2	301	15.5
run	17.9	8.7	1,455	3.5	16.8	9.1	194	10.0
slackwater	33.8	16.4	13,686	33.3	27.7	14.9	445	22.9
slow glide	24.7	12.0	12,981	31.6	19.3	10.4	311	16.0
Total LYR	206.5		41,053		185.9		1,943	

Table 4

Adjacency probabilities between the starting unit (left column) to all other units (top row). Grayed boxes represent values that are much larger than random ( $\sim > 1.6$ ), i.e., a 'collocation'. Values much less than random ( $\sim < 0.4$ ) represent an 'avoidance'. Results shown here include all MU polygons, regardless of size.

	chute	fast glide	pool	riffle	riffle trans	run	slack water	slow glide
chute	--	0.5	0.1	2.8	0.6	3.9	0.0	0.2
fast glide	0.1	--	0.7	0.5	3.2	0.7	0.7	2.3
pool	0.1	2.8	--	0.0	0.3	0.6	1.2	3.1
riffle	0.4	0.4	0.0	--	3.1	1.0	1.1	2.0
riffle trans	0.0	0.7	0.0	0.5	--	0.2	3.0	3.6
run	0.5	2.5	0.6	2.3	1.6	--	0.1	0.3
slackwater	0.0	0.2	0.1	0.2	1.9	0.0	--	5.6
slow glide	0.0	0.6	0.1	0.2	2.1	0.1	4.9	--



Table 5  
Adjacency probabilities between the starting unit (left column) to all other units (top row). Grayed boxes represent values that are much larger than random ( $\sim > 1.6$ ), i.e., a 'collocation'. Values much less than random ( $\sim < 0.4$ ) represent an 'avoidance'. Results shown here include only the MU polygons larger than the minimum size threshold.

	chute	fast glide	pool	riffle	riffle trans	run	slack water	slow glide
chute	--	0.0	0.2	4.1	0.0	3.7	0.0	0.0
fast glide	0.0	--	1.1	0.8	2.5	1.4	0.1	2.1
pool	0.1	2.1	--	0.0	0.0	1.0	2.5	2.3
riffle	1.6	1.0	0.0	--	2.9	2.4	0.0	0.1
riffle trans	0.0	1.6	0.0	1.9	--	1.2	1.1	2.1
run	1.1	1.8	0.9	2.2	2.0	--	0.0	0.0
slackwater	0.0	0.2	1.5	0.1	1.7	0.0	--	4.6
slow glide	0.0	1.6	0.9	0.0	2.2	0.0	3.3	--

Table 6  
 Summary of physical channel characteristics at cross sections associated with each MU type. Bold values represent the maximum within each column and underlined values represent the minimum.

Morphological unit	Water surface slope (%)	Ratio of base flow wetted width to mean width		Bankfull width–depth ratio		
		width	width	Mean	% < 12	% > 40
chute	0.416	<u>0.47</u>	113	0	<b>100</b>	
fast glide	0.038	0.96	73	0	75.3	
pool	<u>0.013</u>	0.93	<u>26</u>	<b>1.2</b>	<u>8.2</u>	
riffle	<b>0.765</b>	0.94	<b>114</b>	0	93.4	
riffle transition	0.124	1.14	89	0	93.6	
run	0.118	0.78	82	0	83.1	
slackwater	0.027	<b>1.58</b>	90	0	91.7	
slow glide	0.030	1.00	64	0	85.7	

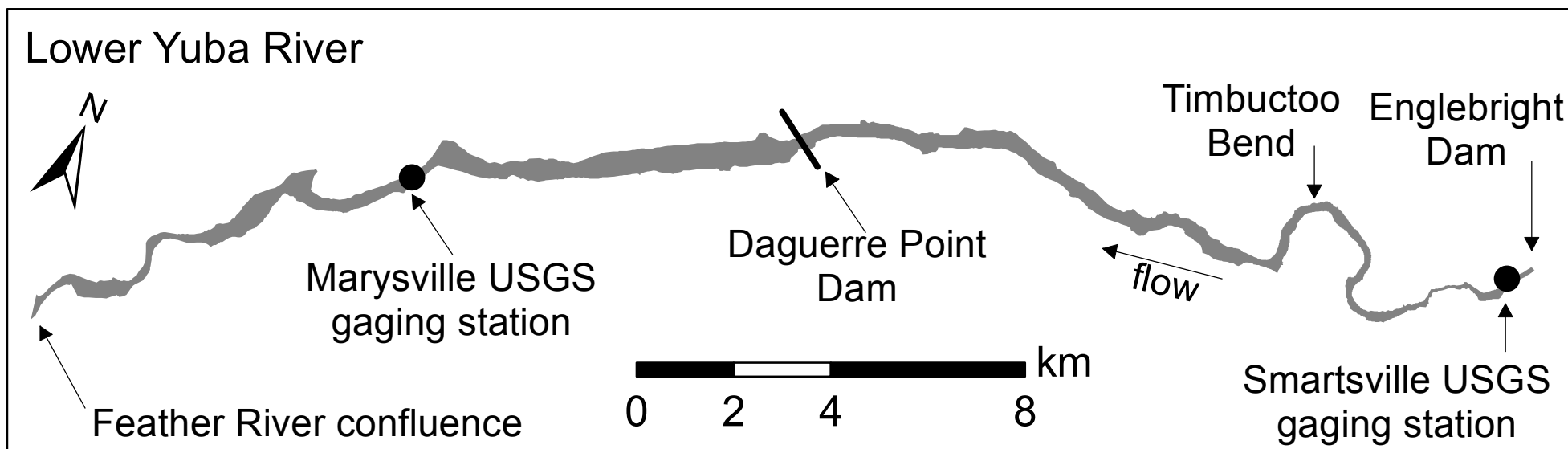
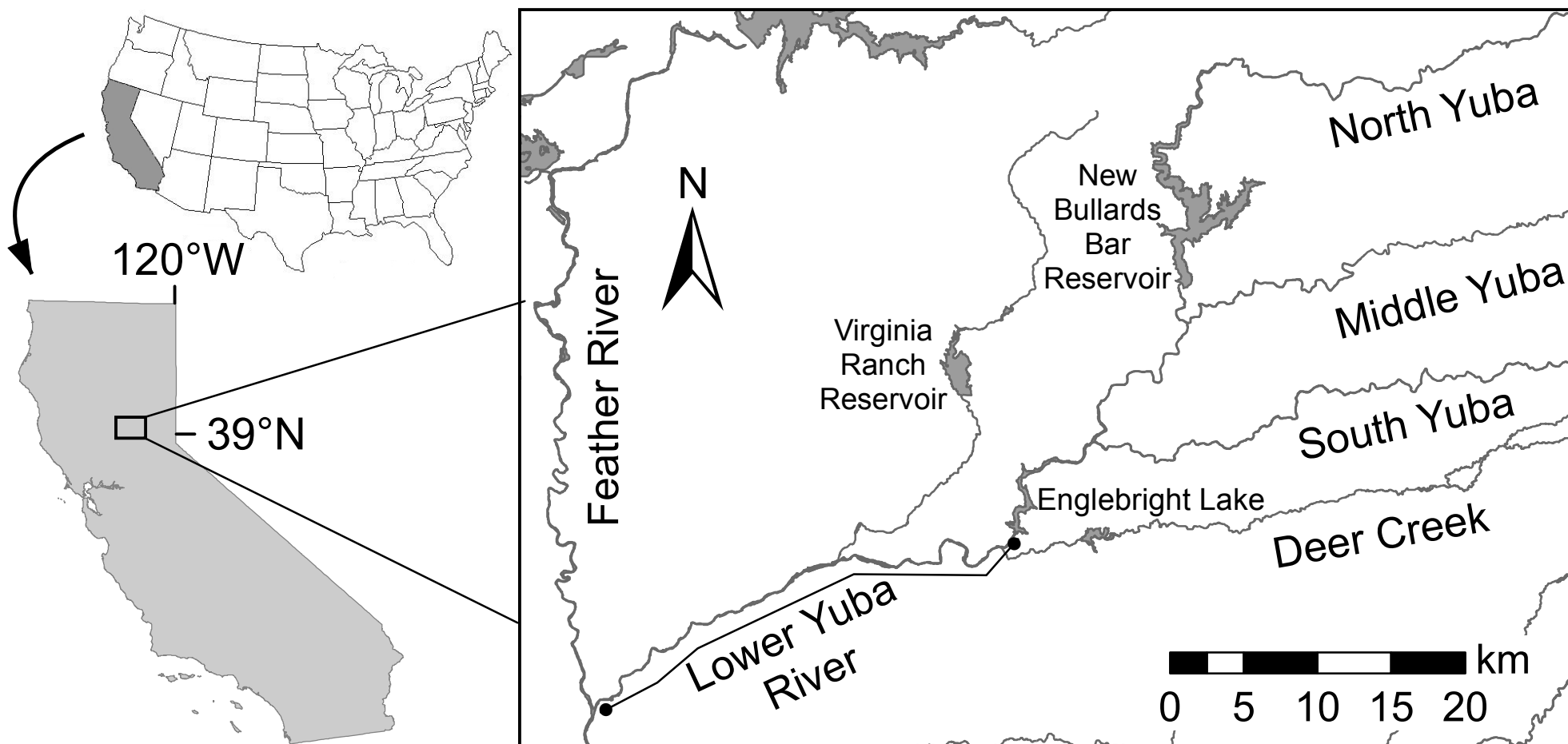
Table 7  
 Comparison of the means and modes for longitudinal spacings between like MUs as normalized by either the mean channel bankfull width or mean channel baseflow width

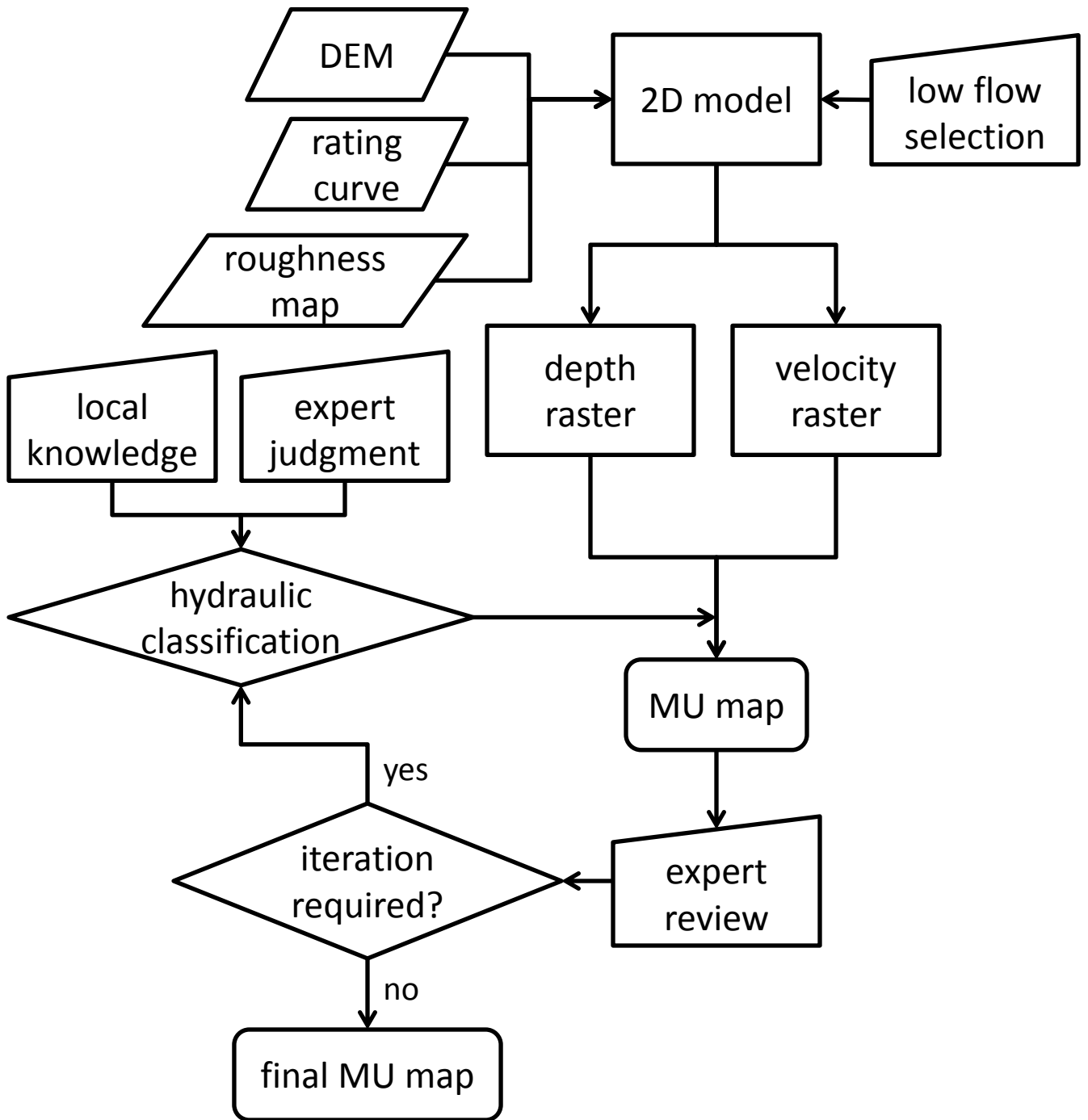
Morphological unit	Normalized by bankfull width		Normalized by base-flow width	
	Mean	Mode	Mean	Mode
chute	4.4	3	7.1	4
fast glide	3.0	2-3	4.9	2-5
pool	4.3	2-5	7.0	3-8
riffle	3.3	2-3	5.4	4
riffle transition	3.2	2-4	5.2	3-4
run	2.7	2	4.3	2-3

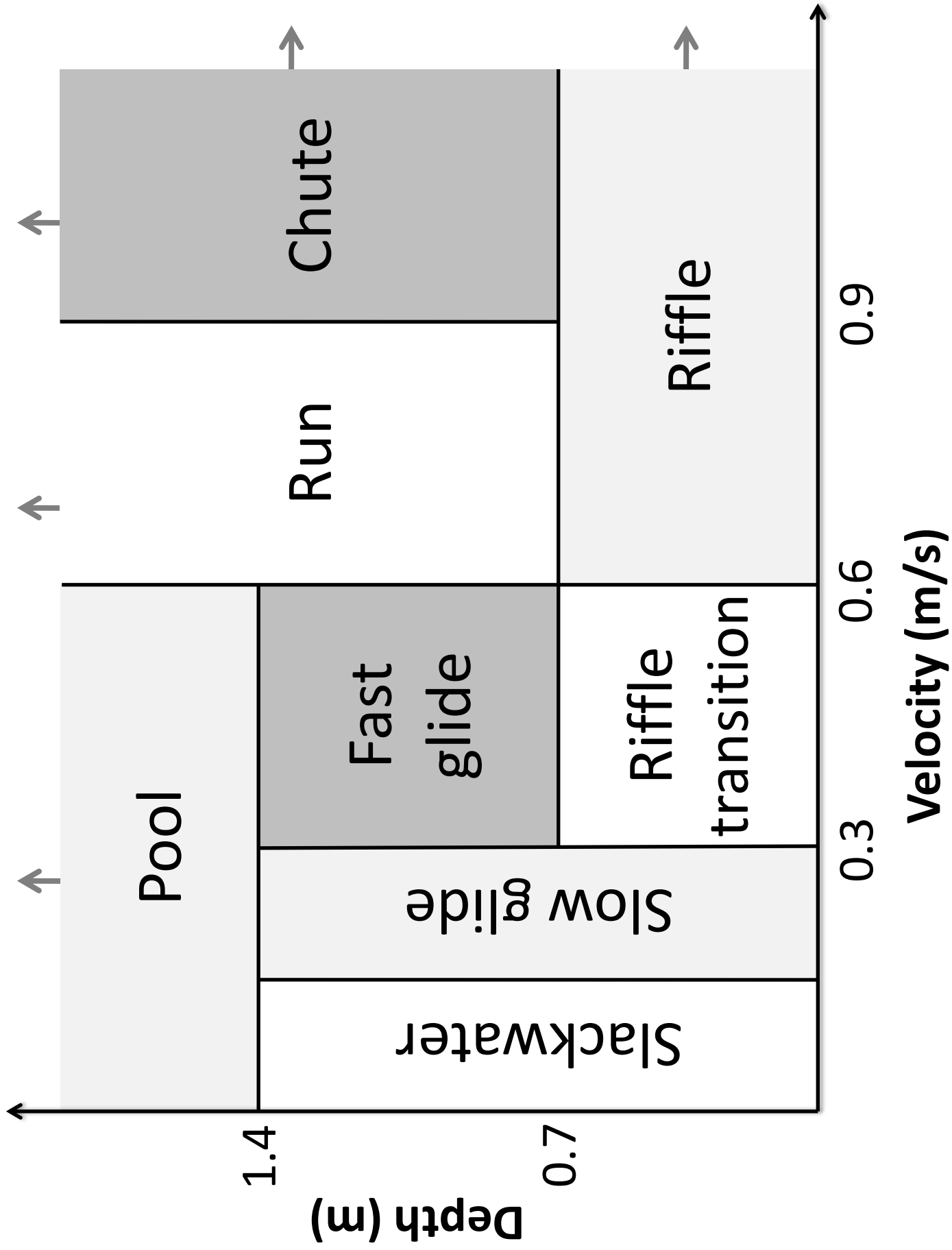
Table 8

Summary of the spatial organizations for each MU, using the minimum size threshold for the polygons. The data in column 2 are synthesized from Table 2; column 3 from Fig. 8; column 4 from Fig. 9; column 5 from Table 4; and column 6 is the average number of other MUs within a cross section that also contains the starting MU.

Morphological unit	Abundance (% segment area)	Longitudinal distribution	Longitudinal spacing (W)	Adjacency (collocation to, avoidance of)	Lateral variability (avg # of other MU per cross-section)
chute	4.5	avoidance near mouth; preference u/s of DPD	4.4	run, riffle <i>all others</i>	4.7
fast glide	14.7	avoidance in u/s bedrock region; preference near DPD	3.0	riffle transition, run, slow glide <i>chute, slackwater</i>	5.0
pool	17.4	avoidance in middle near DPD; preference near mouth and upper bedrock reaches	4.3	fast glide, slackwater, slow glide <i>chute, riffle, riffle trans.</i>	3.8
riffle	13.9	avoidance near mouth and Englebright Dam; preference u/s of DPD	3.3	riffle trans., run, chute <i>pool, slackwater, slow glide</i>	4.7
riffle transition	15.2	avoidance near mouth; preference d/s of DPD	3.2	fast glide, riffle, slow glide, slackwater <i>chute, pool</i>	4.6
run	9.1	avoidance near mouth; preference u/s of DPD	2.7	fast glide, riffle, riffle transition <i>slackwater, slow glide</i>	5.3
slackwater	14.9	no avoidance; some preference d/s of DPD	<i>n/a</i>	riffle transition, slow glide, pool <i>all others</i>	4.1
slow glide	10.4	no avoidance; some preference d/s of DPD	<i>n/a</i>	fast glide, riffle transition, slackwater <i>chute, riffle, run</i>	4.8

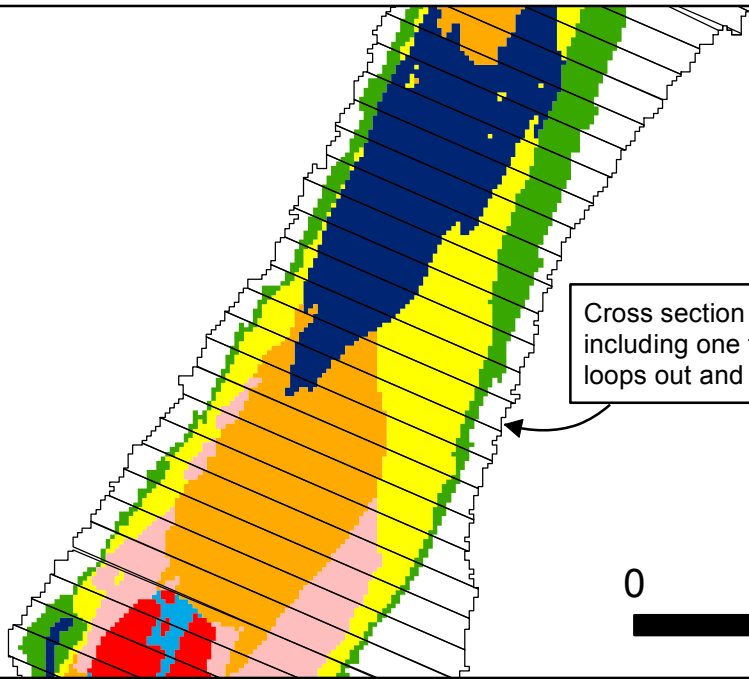




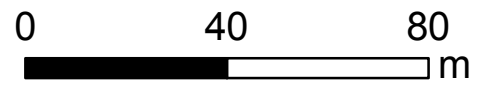


### Morphological units

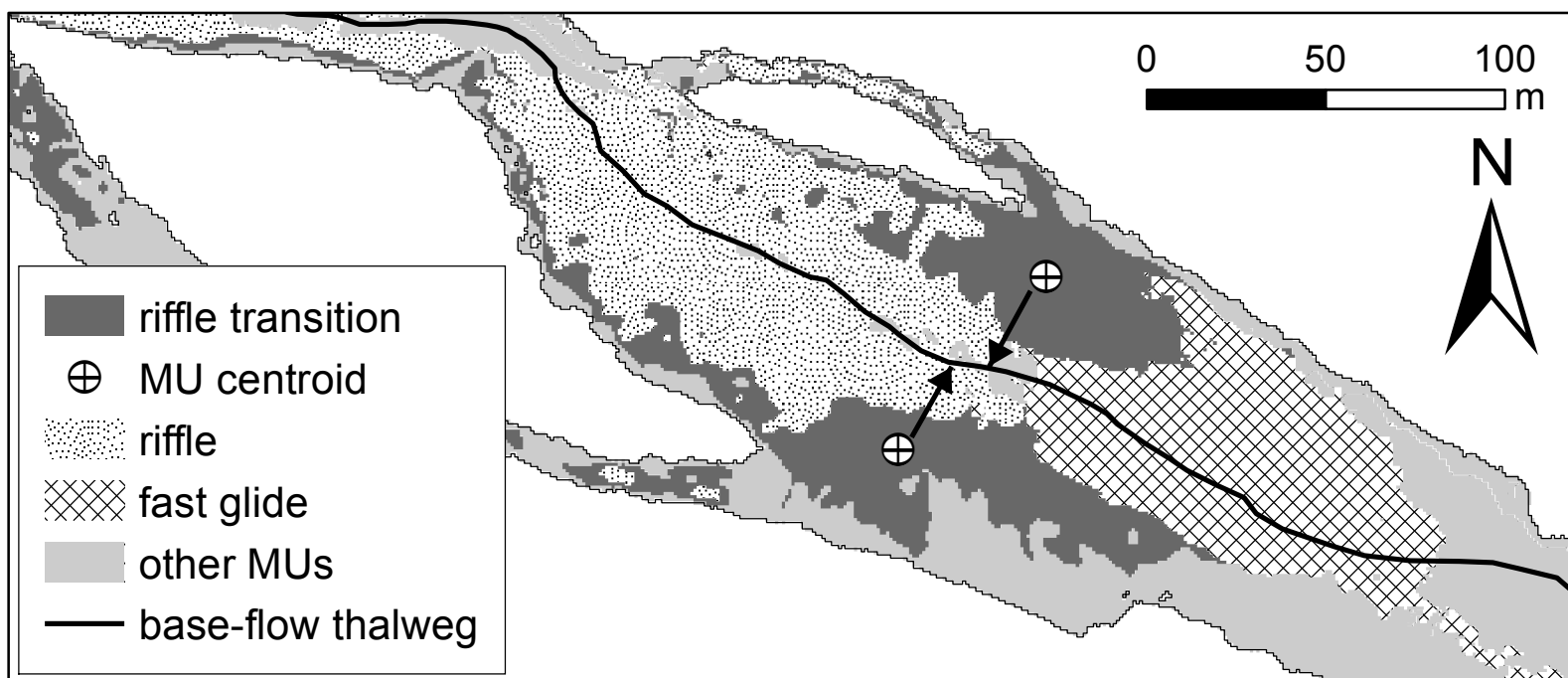
- chute
- fast glide
- pool
- riffle
- riffle transition
- run
- slackwater
- slow glide

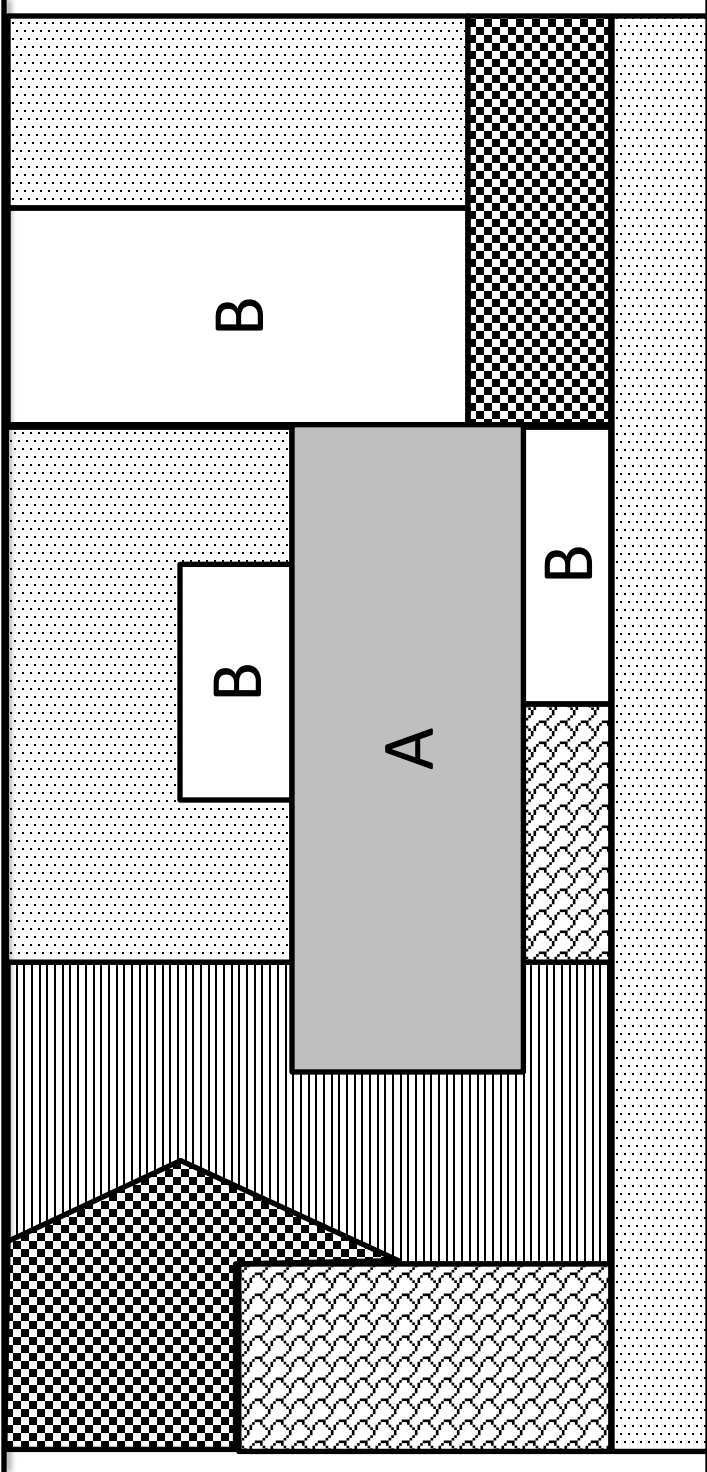


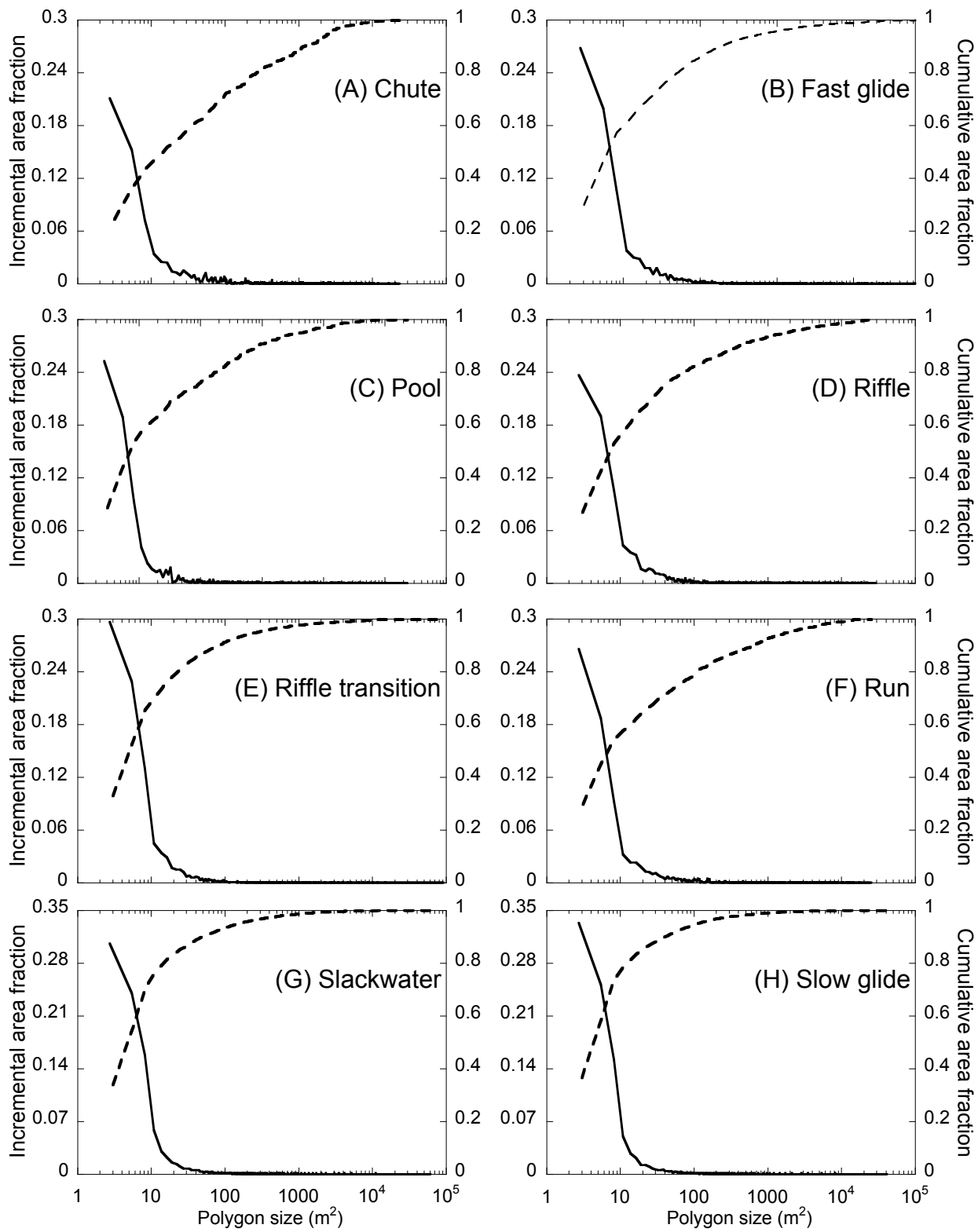
Cross section with six MUs,  
including one fast glide that  
loops out and back in

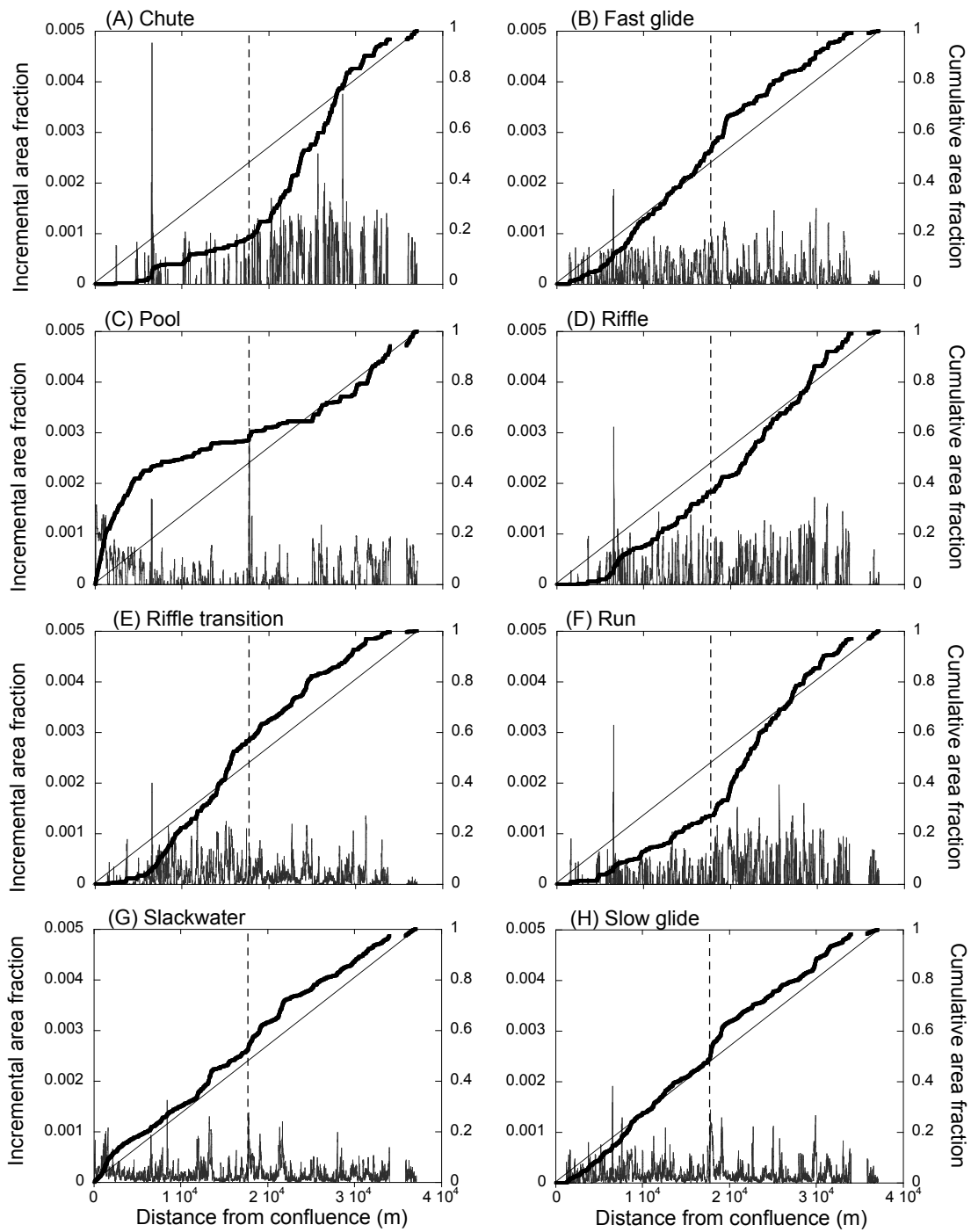


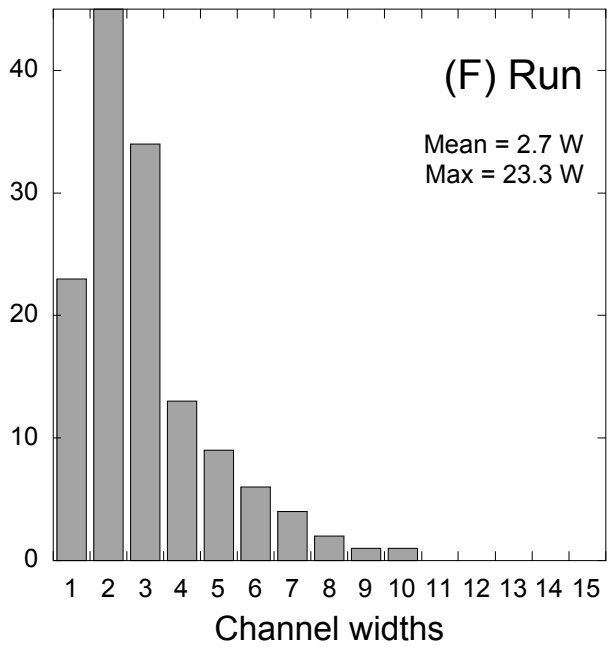
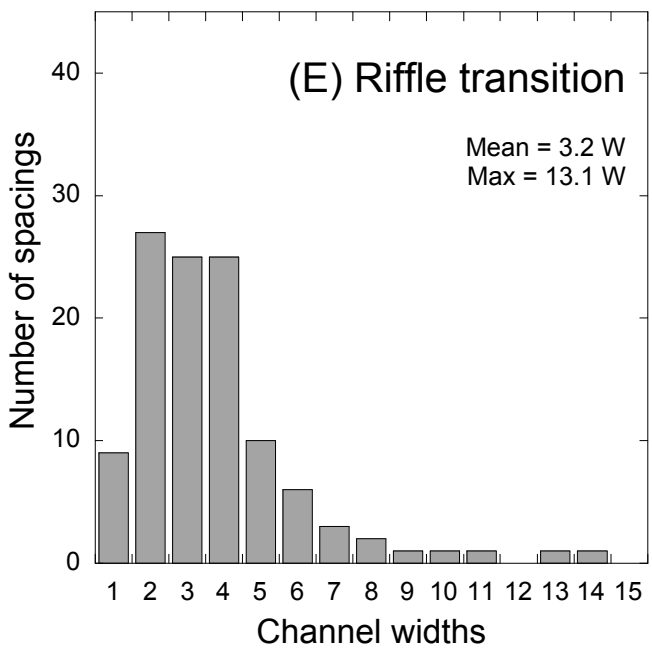
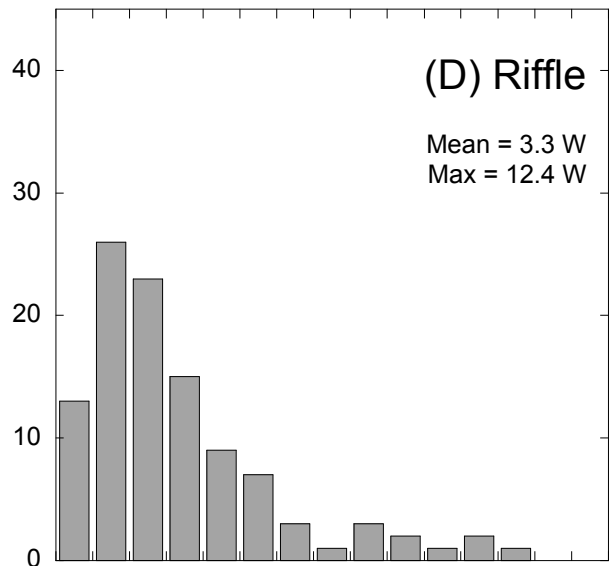
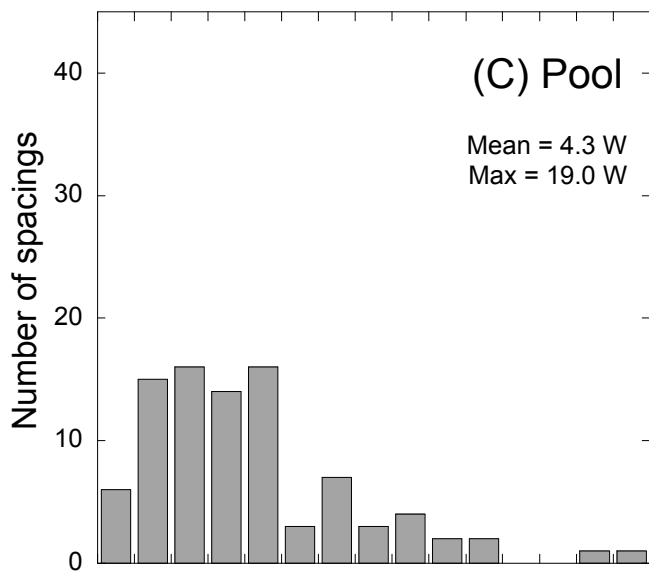
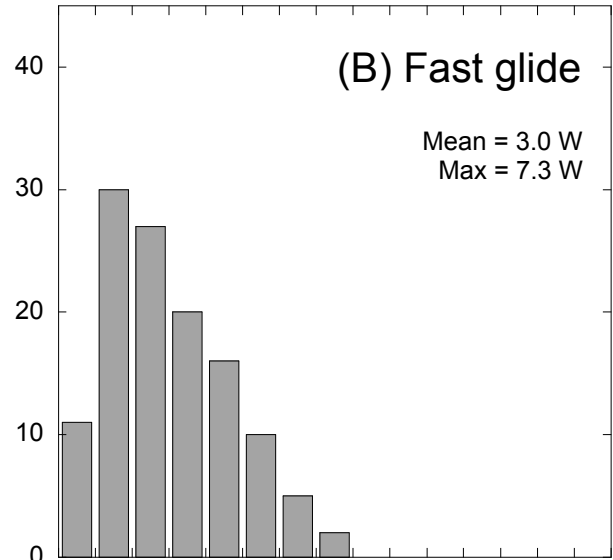
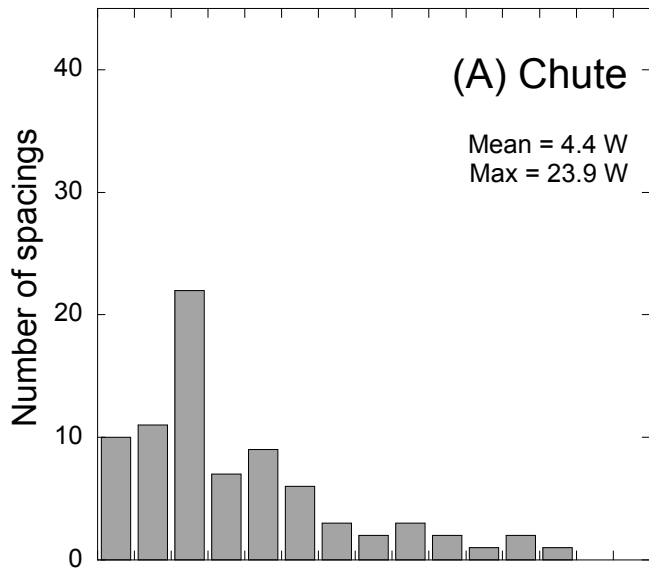




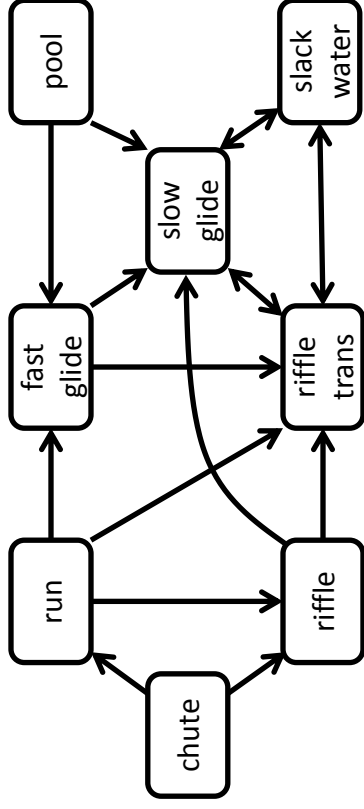




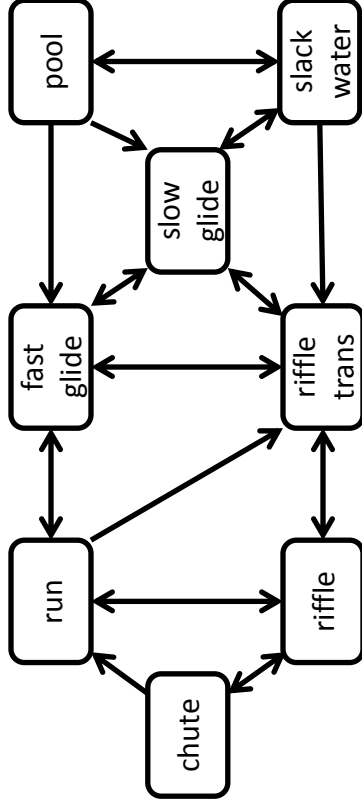


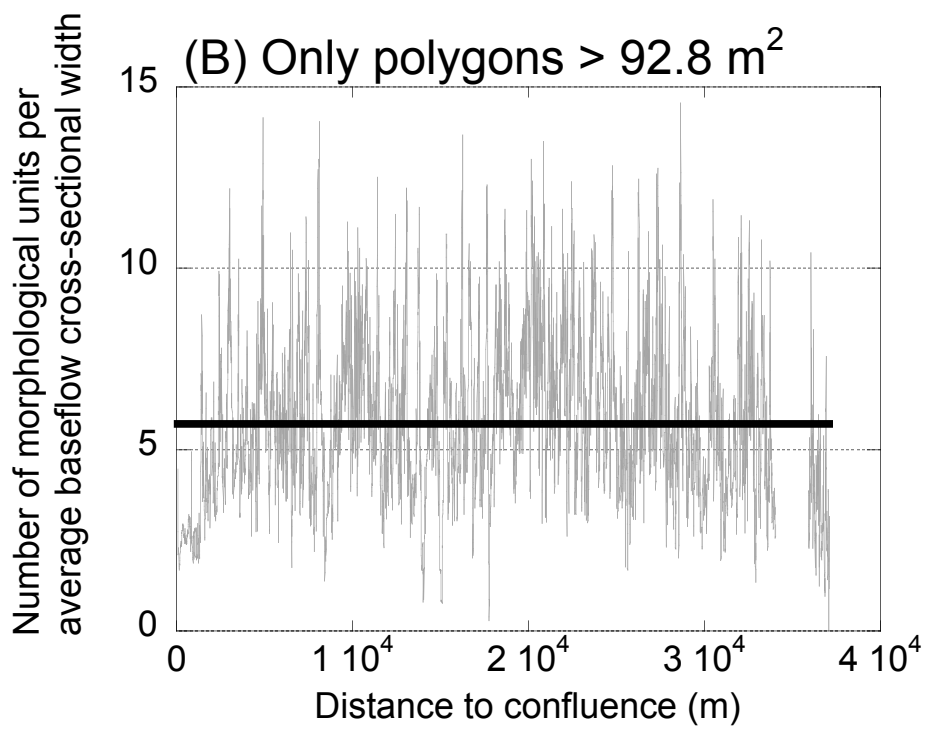
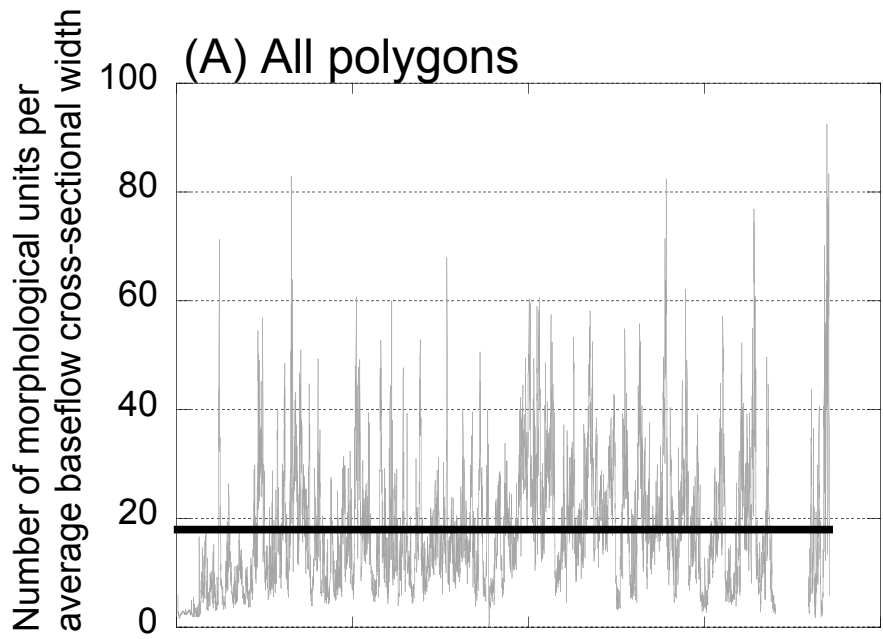


(A) All polygons

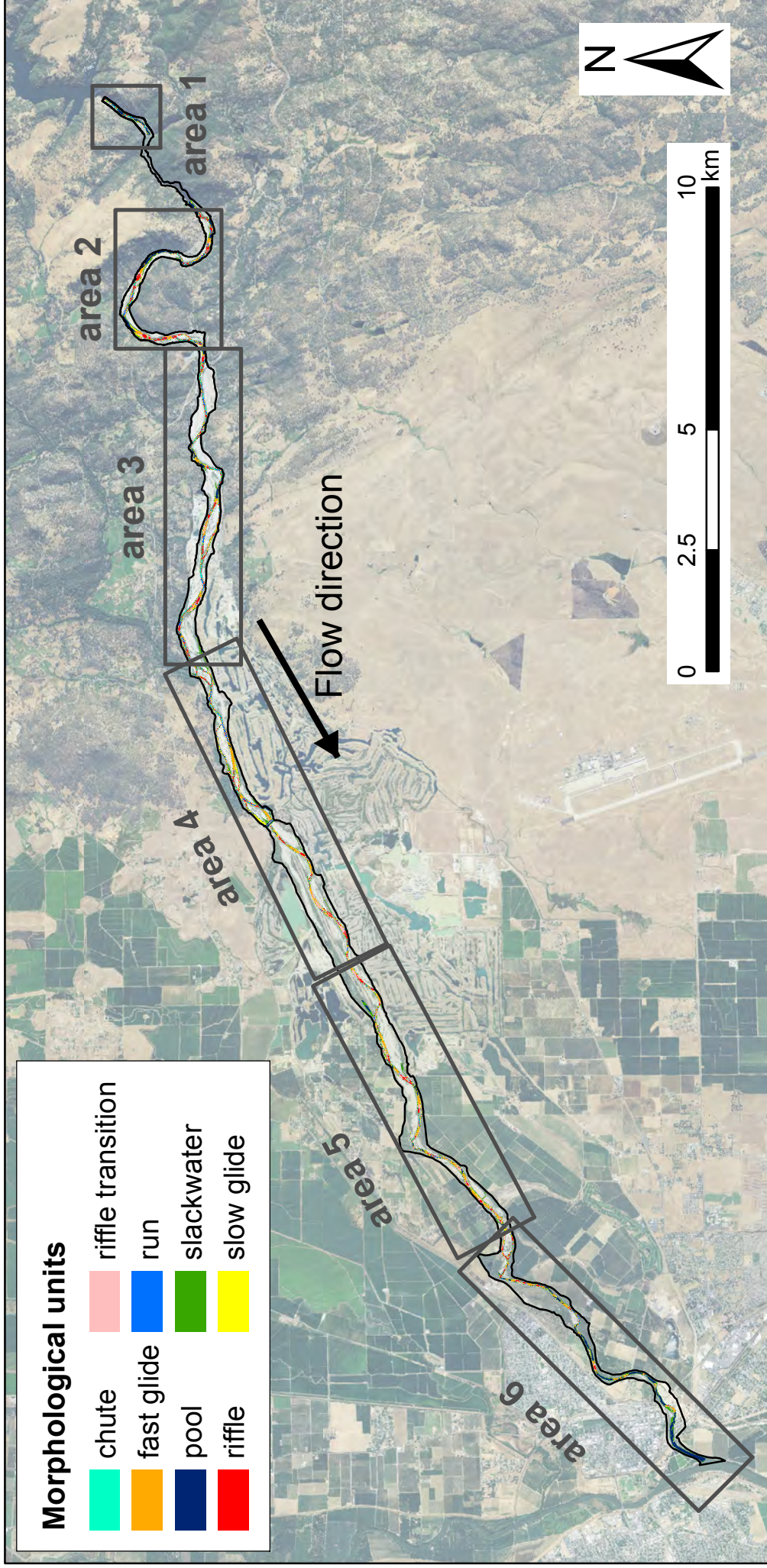


(B) Only polygons > 92.8 m<sup>2</sup>



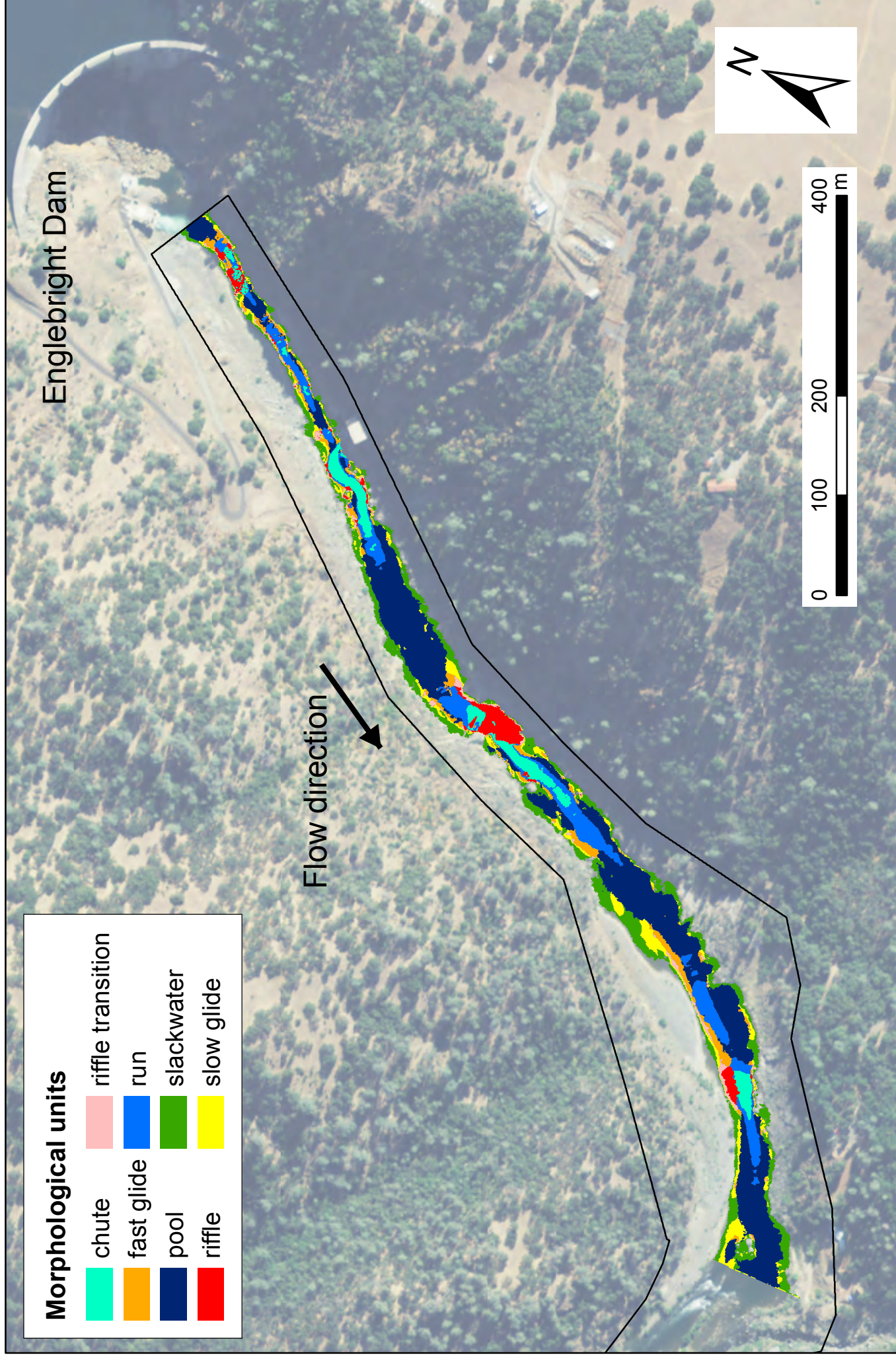


# LYR MU: areal divisions

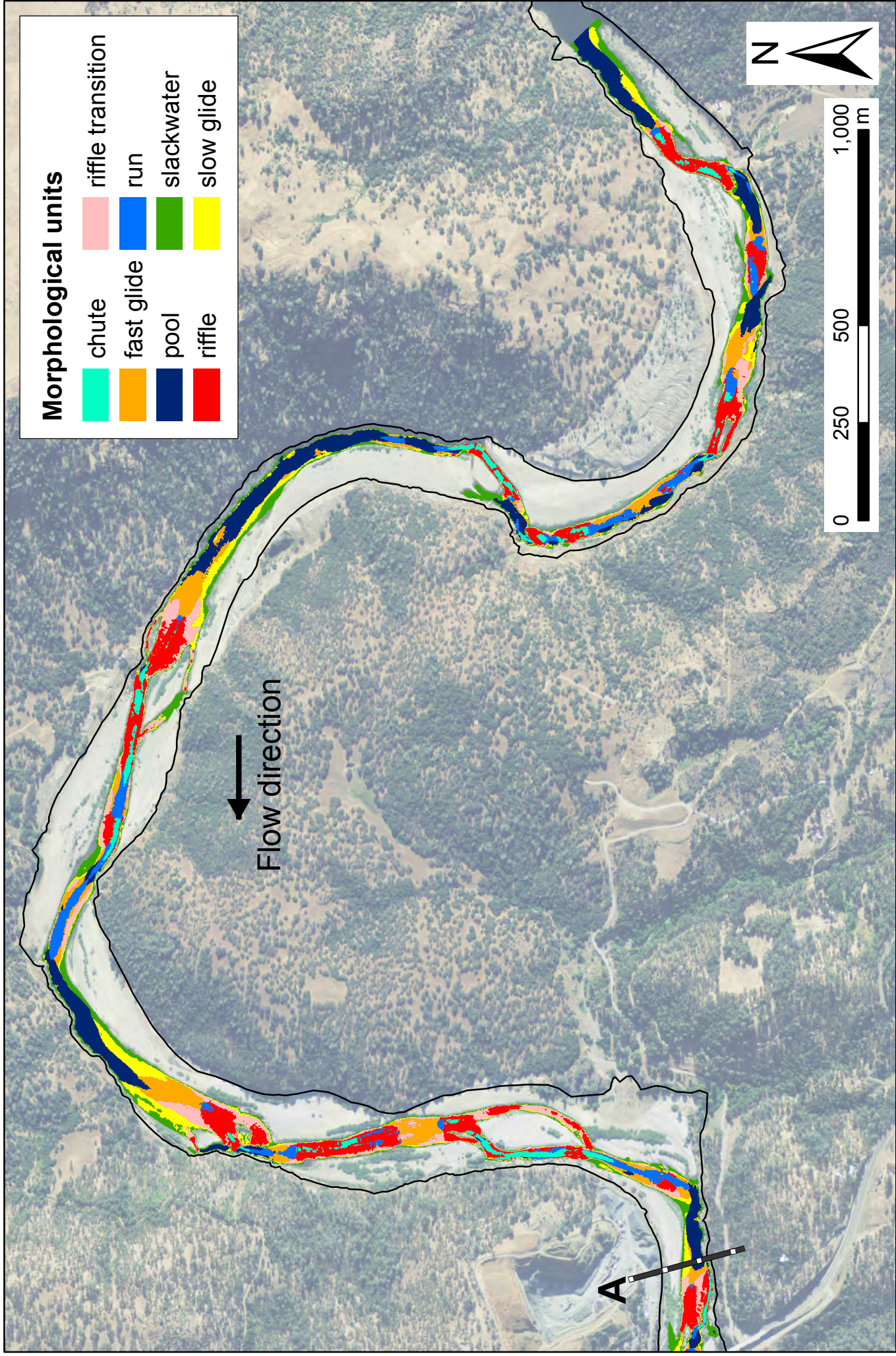




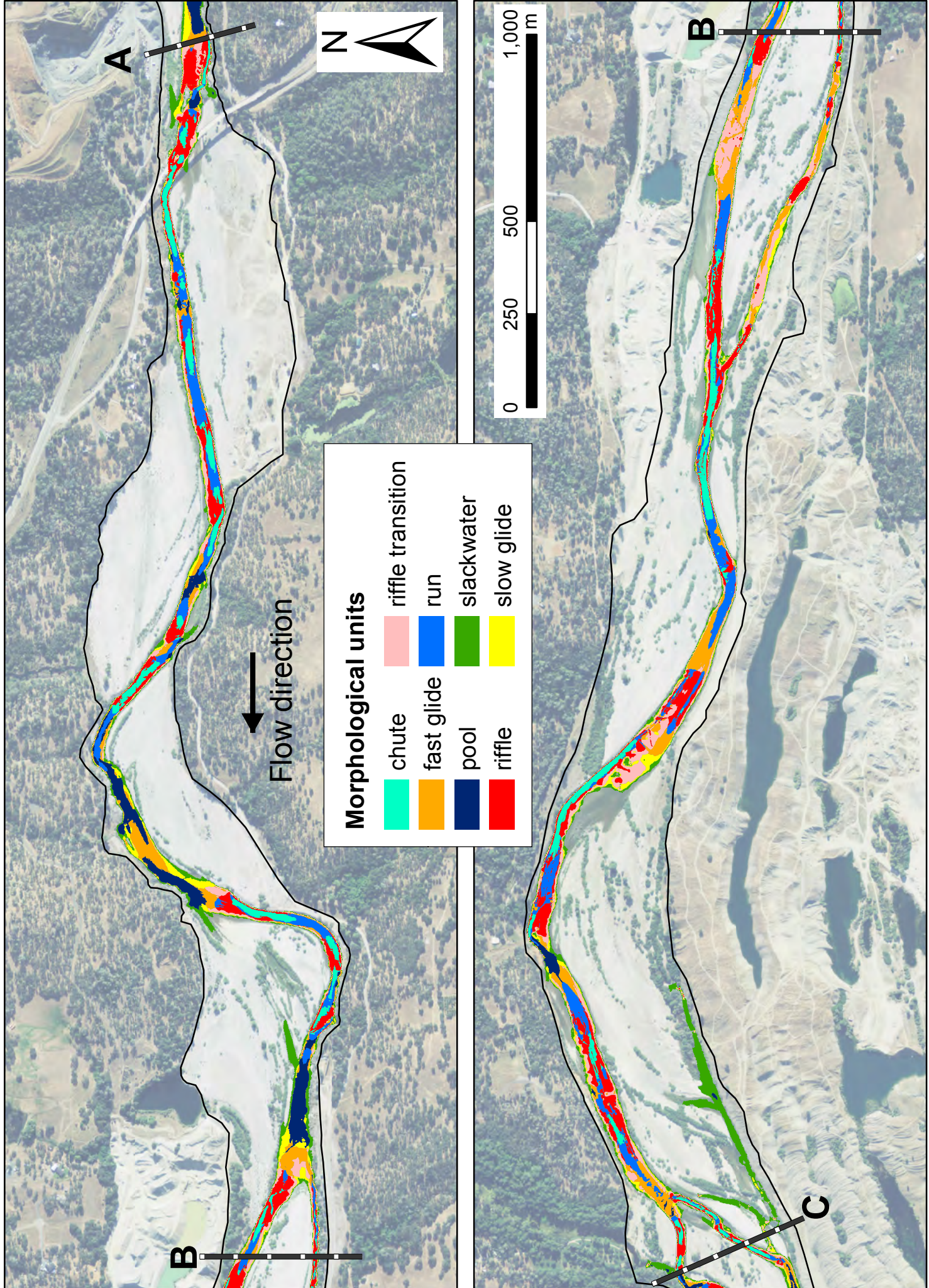
# LYR MU: area 1



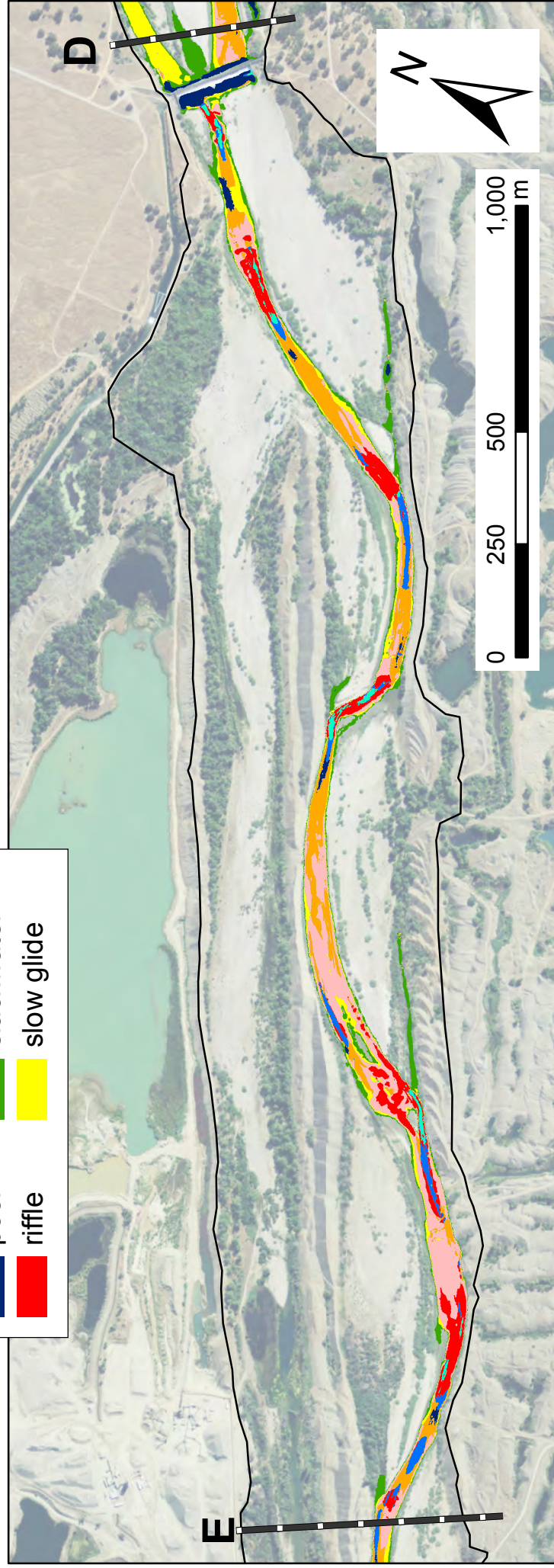
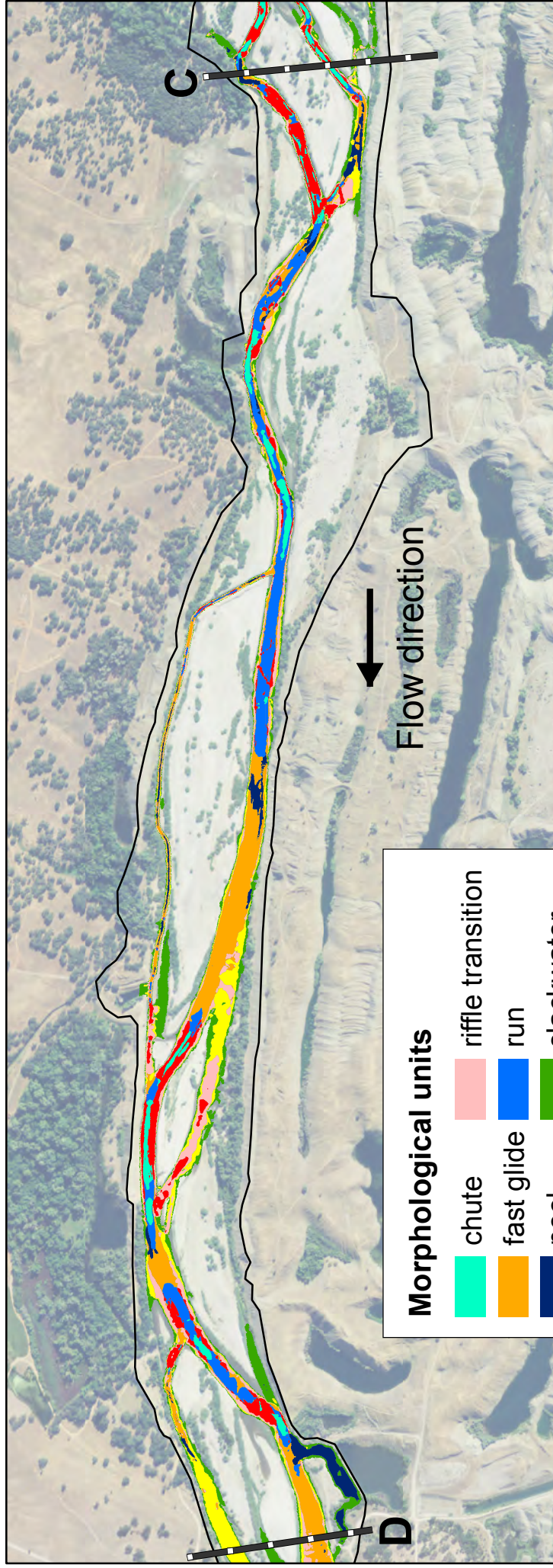
# LYR MU: area 2



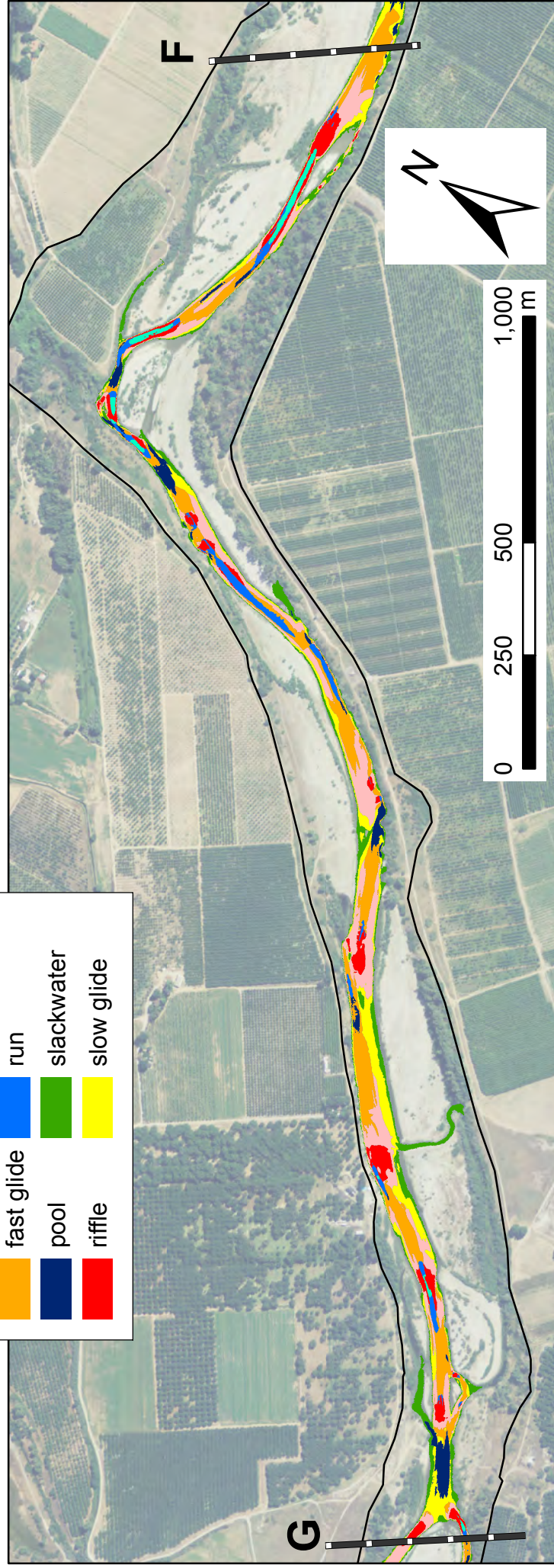
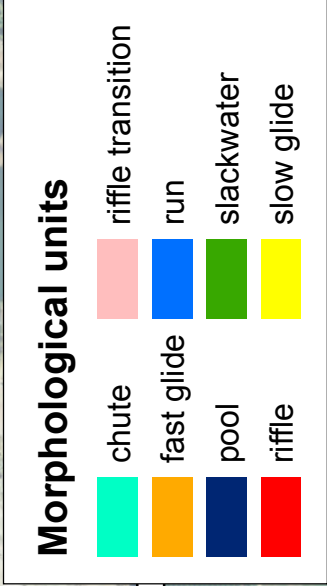
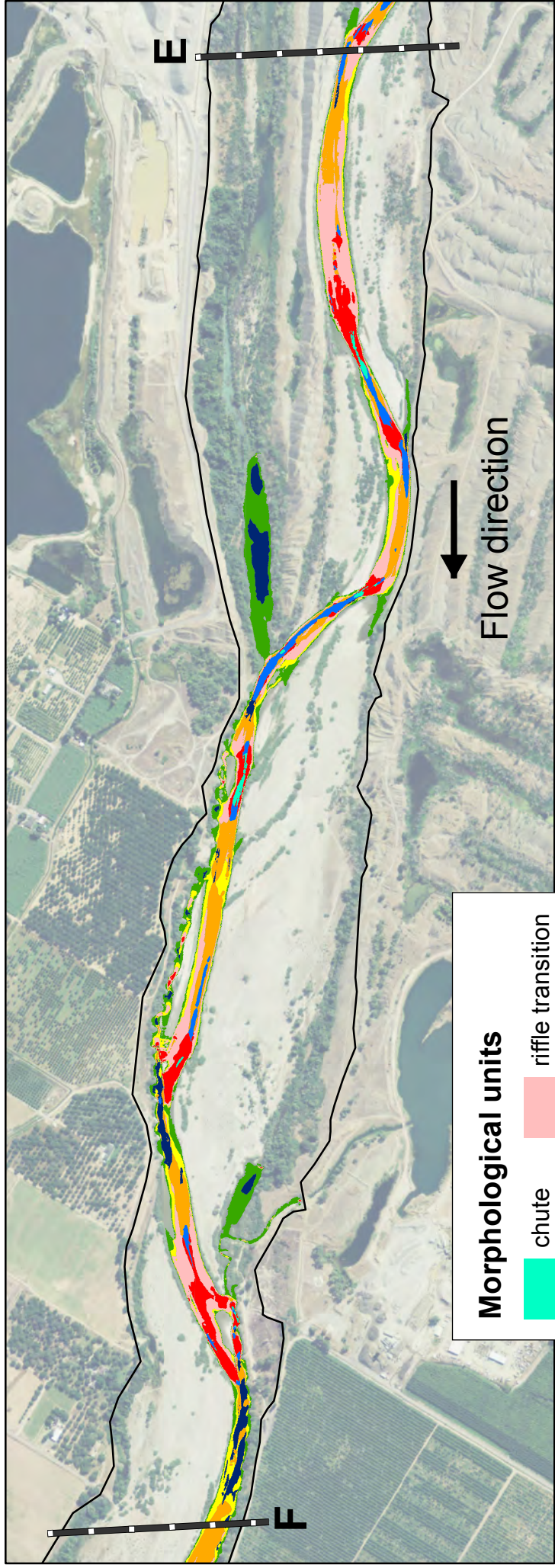
# LYR MU: area 3



# LYR MU: area 4



# LYR MU: area 5



# LYR MU: area 6

